UNIVERSITY OF OKLAHOMA

GRADUATE COLLEGE

IMPROVED SURFACTANT PERFORMANCES IN POROUS MEDIA: EFFECTS OF HYDROTROPES AND BIO-COLSOVENTS

A THESIS

SUBMITTED TO THE GRADUATE FACULTY

in partial fulfillment of the requirements for the

Degree of

MASTER OF SCIENCE

By

NA YUAN
Norman, Oklahoma
2018

Downloaded from SHAREOK. Persistent Handle URL: https://hdl.handle.net/11244/316311

IMPROVED SURFACTANT PERFORMANCES IN POROUS MEDIA: EFFECTS OF HYDROTROPES AND BIO-COLSOVENTS

A THESIS APPROVED FOR THE
MEWBOURNE SCHOOL OF PETROLEUM AND GEOLOGICAL ENGINEERING

BY

Dr. Benjamin Shiau, Chair

Dr. Jeffery Harwell

Dr. Xingru Wu

© Copyright by NA YUAN 2018
All Rights Reserved.

Acknowledgements

I would like to thank all my family member for supporting me, especially my parents, for everything they did to encourage me.

I would like to thank my committee chair Dr. Shiau and my committee member Dr. Harwell and Dr. Wu who helped me with the research work and be my mentor.

I would like to thank all my colleagues at Applied Surfactant Laboratory, for all the help with my research work and train me on the use of laboratory apparatus.

Table of Contents

Acknowledgements iv

List of Tables viii

List of Figures ix

Abstract xiii

Chapter 1. Mitigation of Surfactant losses in porous media: influences of hydrotrope on transport and microemulsionfication. 1

I. Introduction..... 1

Surfactant system 2

Objectives 3

II. Literature review 5

Surfactants 5

Surfactant Flooding 7

Hydrotrope ……...……..….... 9

Phase behavior and HLD Equation 10

R Ratio..... 13

Surfactant Adsorption 14

III. Experimental 16

Materials 16

Methods 17

Phase behavior 18

Coalescence rate 19

Interfacial Tension 19

Adsorption test ……..……...20

Surface tension measurements ……..……23

Stability test 24

IV. Results and Conclusions 25

Phase behavior of Case 1 (Surfactant Only without hydrotrope) 25

Phase behavior of Case 2 (Surfactant with 5% Urea) 31

Phase behavior of Case 3 (Surfactant with Sodium xylene sulfonate) ……. 35

Stability Test 43

Solubilization Parameter 47

Adsorption Study 49

Conclusion 59

Chapter II: Formulations of Microemulsions for Dense Non-Aqueous Phase Liquids: Effects of Soybean Oil Methyl Ester……...……60

Introduction…….…….....……. 60

Bioremediation …….....……...…... 61

Fatty acid methyl esters (FAME) ……62

Dense non-aqueous phase liquid (DNAPL) …….……63

Objective ……...…64

Materials & Methods …….……...……65

Materials ……...…..…. 65

Methods …….....…. 66

Results and conclusions ……...…….…..... 67

Prediction of the equivalent alkane carbon number (EACN) ……...67

Density alteration of SoyGold and TCE mixture …….……...… 71

Phase behavior study of SoyGold 1100 and TCE mixture ……...72

Stability test with Viscosity measurements…….……73

Conclusion ……...…75

References 76

List of Tables

Table 1: Properties of Four types of Pure Alkane Hydrocarbon……..... 16

Table 2: Summary of Phase Behavior of Case 1 (Surfactant only) 45

Table 3: Summary of Phase Behavior of Case 2 (with urea) 46

Table 4: Summary of Phase Behavior of Case 2 (with NaXS) 46

Table 5: Adsorption Reduction by Adding Urea 54

Table 6: Adsorption Reduction by Adding NaXS 55

Table 7: Comparisons of various SoyGold Products…….……..…… 65

Table 8: Hydrocarbons Tested …….……..…. 65

Table 9: Density adjustment of SoyGold and TCE mixture ……....……. 71

Table 10. Viscosity measurements in centipoises…….…….. 74

List of Figures

Figure 1: Chemical Structure of AOT (top), SDBS (bottom left) and urea (bottom right) and Sodium Xylene Sulfonate (bottom middle) ……....3

Figure 2: Schematic Illustration of Basic Structure of Surfactant. 6

Figure 3: Schematic Illustration of Three Main Types of Micelle Shapes (Som et al. 2012). ……...…… 6

Figure 4: Schematic illustration of the various types of surfactants (Roland.chem, 2006) …….……..…. 7

Figure 5: Mechanisms of Surfactant Flooding (Abriola, 2002) 8

Figure 6: Variation in interfacial tension versus water salinity (Jin et al. 2017) ....…..... 12

Figure 7: Illustration of R Ratio Corresponding to Typically Observed Phase Behavior (Salager and Antón 1999) 14

Figure 8: Thermo Scientific: Genesys 10s UV-VIS Spectrophotometer……. 21

Figure 9: Calibration of Absorbance for SDBS only (top) and SDBS with 5% Urea (bottom) on 190 to 300 nm Wavelength 22

Figure 10: Attension Theta Optical Tensionmeter..... 24

Figure 11: Attension Theta Optical Tensiometer Operation Software (Biolin Scientific) 24

Figure 12: Salinity scan for Case 1 with Heptane 26

Figure 13: Salinity scan for Case 1 with Octane..... 26

Figure 14: Salinity scan for Case 1 with Decane 27

Figure 15: Salinity scan for Case 1 with Dodecane 28

Figure 16: Natural log of salinity vs. EACN for Case 1(Surfactant with DI Water) optimum points 29

Figure 17: IFT vs. salinity for Case 1(Surfactant with DI Water) 30

Figure 18: EACN vs. Salinity for Case 1 with microemulsion type identified 30

Figure 19: Salinity scan for Case 2 with Heptane 31

Figure 20: Salinity scan for Case 2 with Octane 32

Figure 21: Salinity scan for Case 2 with Decane 32

Figure 22: Salinity scan for Case 2 with Dodecane ……..……. 33

Figure 23: Salinity vs. EACN for Case 2 optimum points ……...33

Figure 24: IFT vs. salinity for Case 2 34

Figure 25: EACN vs. Salinity for Case 2 with microemulsion type 34

Figure 26: Salinity scan for 5% NaXS with Heptane at room temperature ….....…….. 36

Figure 27: Salinity scan for 5% NaXS with Heptane at 50°C 37

Figure 28: Salinity scan for 1% NaXS with Heptane at room temperature 38

Figure 29: Salinity scan for 1% NaXS with Heptane at 50°C..... 39

Figure 30: Example of Surfactant Sample contains 1% NaXS, 0.6% NaCl and Heptane at 50°C..... 40

Figure 31: Salinity scan for 0.5wt% NaXS with Heptane at Room Temperature (upper) and 50°C (lower). 41

Figure 32: Salinity scan for 0.1wt% NaXS with Dodecane at Room Temperature (upper) and 50°C (lower)…….…… 42

Figure 33: Stability Test Samples with 0.75% AOT, 0.19% SDBS and NaCl. Surfactant only (top), with 5% urea (middle) and 1% NaXS (bottom)…… 43

Figure 34: Example of Precipitation Sample of Stability Test …….….. 45

Figure 35: Solubilization Parameter and Interfacial Tension of AOT and SDBS with 5% Urea Mixed with Decane…….....…….48

Figure 36: Comparison of Ottawa sand (left), Indiana limestone (middle) and Activated Carbon (right)…….....…….……50

Figure 37: Comparison of Activated Carbon Samples Pre (Top) and Post (bottom) Adsorption……..…… 51

Figure 38: Comparison of Ottawa Sand Samples Pre (Top) and Post (bottom) Adsorption…….…….….52

Figure 39: Adsorption Test of SDBS with Ottawa Sand…….……53

Figure 40: Adsorption Test of SDBS with Indiana limestone.…….....…53

Figure 41: Adsorption Test of SDBS with Activated carbon.....…….54

Figure 42: Surface Tension Measurement SDBS with DI and SDBS with 5% urea and 1% NaXS added, measured by pendant drop method…… 57

Figure 43: Droplet of SDBS with NaXS Solution on the Needle surface……..... 58

Figure 44: Illustration of SoyGold Working Process During the Groundwater Bioremediation (Gundling). ……...…… 61

Figure 45: The reaction of producing FAME (European Biofuels) …… 62

Figure 46: The mobility characteristics of DNAPL. Mobile and potentially mobile DNAPL(left) and Immobile residual phase DNAPL(right) (ITRC 2015) …….. 63

Figure 47: Phase behavior samples of SoyGold 1000 for EACN measurement in bigger salinity scan (top) and finer salinity scan (bottom). ……..…….. 67

Figure 48: Phase behavior samples of SoyGold 1100 for EACN measurement…….….68

Figure 49: Phase behavior samples of SoyGold 2000 for EACN measurement……..... 68

Figure 50: IFT measurement of phase behavior sample of SoyGold 1100 and dodecane……. 69

Figure 51: Phase behavior samples of TCE and Octane for EACN measurement…….. 70

Figure 52: Phase behavior samples of SoyGold 1100 and TCE mixture……. 72

Figure 53: IFT measurement of phase behavior samples of SoyGold 1100 and TCE mixture…….……... 73

Figure 54: Stability test samples with 5mL SoyGold 1100 …….……...….73

Figure 55: Stability test samples with 5mL SoyGold 1100 and 2mL TCE…….....74

Abstract

Surfactant flooding for the mobilization of residual oil is a promising technology for enhanced oil recovery (EOR) and surfactant enhanced aquifer remediation (SEAR). A significant economic barrier to the widespread use of the technology is the loss of surfactant through adsorption on aquifer and reservoir minerals. Especially in the case of EOR in highly saline brines, adsorptive losses of surfactant may be the single essential expense in the application. In this study, we examine the use of hydrotropes to reduce surfactant adsorption and to improve the surfactant flooding performance. The HLD equation, interfacial tension measurement and phase behavior of salinity scan were used to determine the Winsor type III microemulsion on four types of pure alkane hydrocarbons. Linear mixing rule has also is utilizing during the analysis. A new method has been established for the detection of hydrotropes, which is using the UV-VIS spectrophotometer on a targeted wavelength range. Adsorption amount is measured and compared within three types of sand materials.

CHAPTER 1. MITIGATION OF SURFACTANT LOSSES IN POROUS MEDIA: INFLUENCES OF HYDROTROPE ON TRANSPORT AND MICROEMULSIONFICATION

I. Introduction

Surfactant flooding is a promising approach in the enhanced oil recovery (EOR) due to its high efficiency of reducing the interfacial tension between oil and water and mobilizing the residual oil (Bera et al. 2013). However, adsorption of surfactant onto reservoir rock surface may cause the loss of surfactant or reduce the surfactant concentration and result in drastic underperformance of surfactant flooding (Bera et al. 2013). Furthermore, excessive adsorption of surfactant in the porous media may cause an economic issue of field operations and severe impact of project investment and return.

This study offers insights on the extent to which addition of proper hydrotrope may help in the reformulation tasks aiming at more efficient and cheaper surfactant flooding candidates. Ideally, this will facilitate to further mitigate the undesirable surfactant losses and improve the surfactant formulations performance for surfactant flooding technology applied in areas of enhanced oil recovery (EOR) and surfactant enhanced aquifer remediation (SEAR). Several of the modified formulations tested could noticeably form a stable and broader Winsor Type III microemulsion region and much relaxed salt window for system optimization, in particularly for oil of longer carbon chain like dodecane. It is anticipated that by adding appropriate hydrotrope in various surfactant system, one can potentially alter the key parameters in the current

flushing system, such as interfacial tension, optimum salinity, coalescent rate, stability and so on, lead to better and cost-effective operations for oil production and contaminant remediation.

Surfactant system

In this study, a binary surfactant mixture system is examined. It contains dual anionic surfactants, dioctyl sodium sulfosuccinate (AOT) and sodium dodecyl benzene sulfonate (SDBS), with the fixed concentration of 0.75% and 0.19% by weight percentage. SDBS is a high content surfactant with noticeable properties of good detergency, moistening, foaming, and dispersity. The biological degradability of SDBS is more than 90% under aerobic conditions. International security organizations have been recognized it as safe chemicals (Qingdao). Urea and Sodium Xylene Sulfonate are the representative hydrotropes used. The chemical structure of these surfactants and hydrotropes are shown in **Figure 1.**

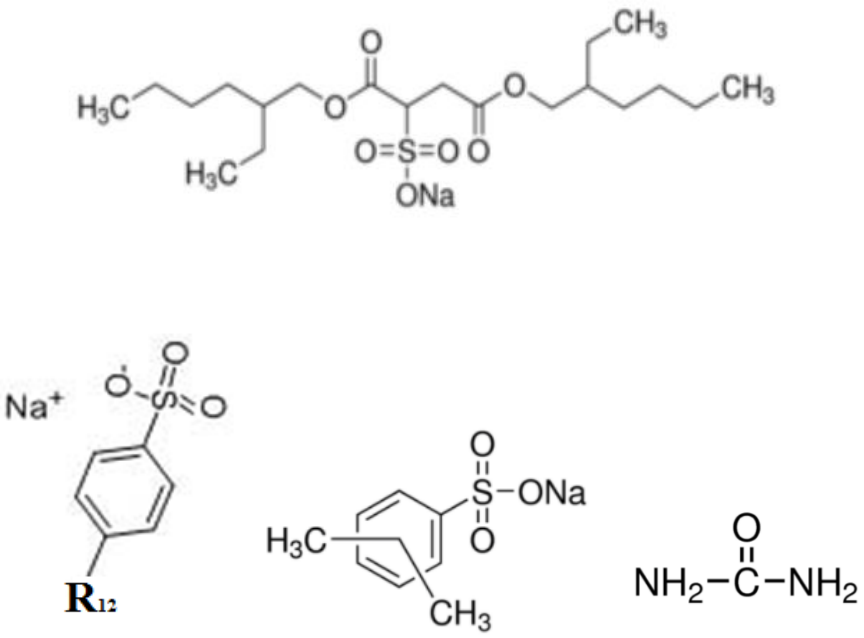

Figure 1: Chemical structure of AOT (top), SDBS (bottom left) and urea (bottom right) and Sodium Xylene Sulfonate (bottom middle)

Objectives

The newly modified system, which the selected hydrotrope was added into the current ultra-low IFT surfactant formulations, could potentially create an improved stable microemulsion with an ultra-low IFT, which can be measured experimentally based on a series of phase behavior study and IFT measurements. In general, an ultra-low IFT system should preferably be

10^{-3} mN/m or less, and the equilibrated samples of Winsor Type III microemulsions should be distinctly recognized with visual observations. Ideally, the targeted total surfactant concentration should be less than one weight percent to meet the environmental requirements and better control of surfactant cost. Most of the key

operational parameters, e.g., optimum salinity, Type III windows, coalescent rate, and stability of the surfactant solutions should show some evidences of improvement.

As for the adsorption study, batch adsorption experiments of sodium dodecyl benzene sulfonate (SDBS) were evaluated in different porous media, involving surfactant contact with Ottawa sand, Indiana limestone and activated carbon for comparison purpose. By adding hydrotrope into the samples, the modified flushing formulations is anticipated to produce a noticeable reduction of surfactant losses on the surfactant adsorption amount. The adsorption amount of surfactant is calculated by comparing the initial and final concentration in the treated solution. In general, after 72-hours of equilibrated period, the concentration of SDBS in the supernatant can be detected simultaneously by two separate devices, ultraviolet-visible spectroscopy (UV-Vis), and High-Performance Liquid Chromatography (HPLC) to cover different concentration levels and sensitivity needs. Results of adsorption plots and their analysis which are exposed to both with and without hydrotrope condition are discussed. Reduction of adsorption amount is calculated and shown in the result section.

II. Literature review

Surfactant

"Surfactant" is a word stand for the surface-active agent which is also the general definition of surfactant. The prevailing impression we have on a typical surfactant in daily life is soap and soap solution can easily generate foam. Surfactant is a type of compound that can be surface active and lower the surface tension or interfacial tension. The surfactant has extensive applications in our life and various industries. In our daily life, surfactants can be found in the dishwasher detergents or personal care products like facial cleanser; it helps water to remove the dirt or the oil from the dishes and our skin surface. It serves the functions of cleaning, wetting, dispersing and emulsifiers (Nippon). In applying chemical flooding for Enhanced Oil Recovery (EOR) technique, surfactants are used to dramatically lower the interfacial tension between oil and water and then achieve the goal of mobilizing the entrapped residual oil.

The basic structure of surfactant contains a hydrophilic(water-loving) head group and a hydrophobic (water-hating) tail group. The general structure of surfactant is shown in the **Figure. 2** below. When mixing with water and oil phase, surfactant head is attracting to the water phase, while the tail group is contacting the oil phase like shown in the figure below. When the surfactant concentration increases and reaches the Critical Micelle Concentration (CMC) the micelle is formed, and its morphology can be a spherical structure, a cylindrical micelle or a bilayer configuration as shown in **Figure. 3**. After forming micelles, the oil phase or the solid dirt will be removed easily; this is also a process of surfactant cleaning, or detergency.

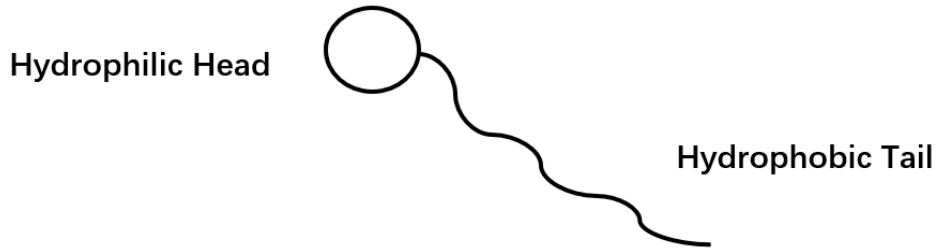

Figure.2. Schematic Illustration of Basic Structure of Surfactant.

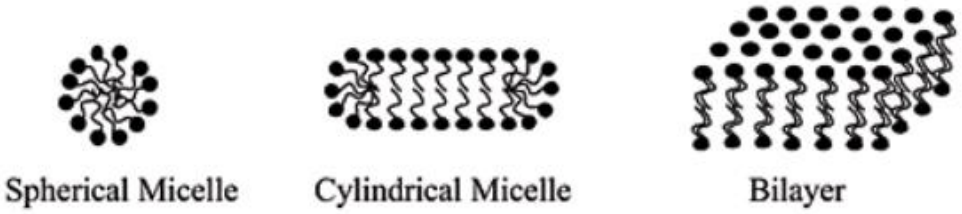

Figure. 3. Schematic Illustration of Three Main Types of Micelle Shapes (Som et al. 2012)

As for the classification of surfactant, the most well-known types are non-ionic, anionic, cationic and amphoteric surfactant. Since the charged part of the surfactant is the polar head group, nonionic surfactant means the head group is not indicated any charges, while the anionic and cationic means the head group can be either negative or positive charge. Amphoteric surfactant also known as the zwitterionic surfactant, this type of surfactant is less common when compare with other three types. Zwitterionic surfactant will show the characteristics of both anionic and cationic surfactant (Som et al. 2012). The illustration of four types of surfactant head group is present below corresponding to various charges of the head group as adopted from the example post from Lorna corp. (Lorna 2018).

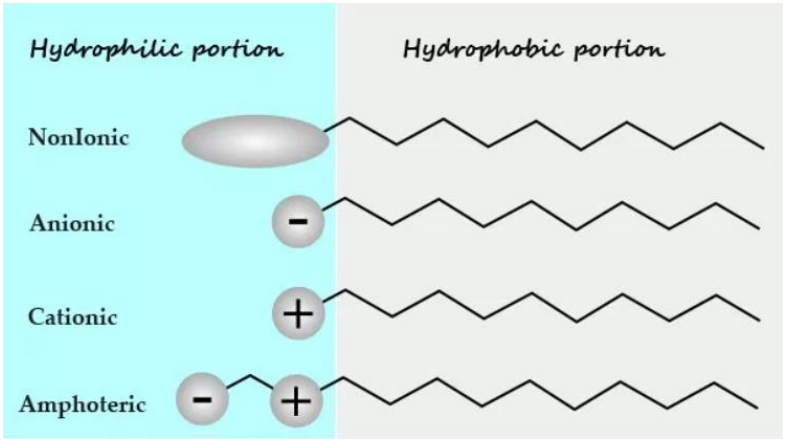

Figure.4: Schematic illustration of the various types of surfactants (Lorna 2018)

Surfactant flooding

Waterflooding is the widely used techniques in the oil fields. However, some oil called residual oil will remain trapped and unproduced in porous media after extended period of waterflooding (Sheng 2015). Residual oil is trapped largely due to strong capillary forces in porous media. Thus, in the Enhanced Oil Recovery (EOR) technique, surfactant flooding is needed to mobilize the residual oil trapped in the reservoir rock by significantly reducing the interfacial tension between oil and water (at least 2 to three orders of magnitude reduction). Two principal operational functions of the injected surfactants are to decrease interfacial tension and promote wettability alteration, especially in the case of carbonate reservoirs (Sheng 2012). The simplified illustration is shown in **Figure 5** below illustrating simple explanation of main mechanisms involved during the surfactant flooding in the reservoir.

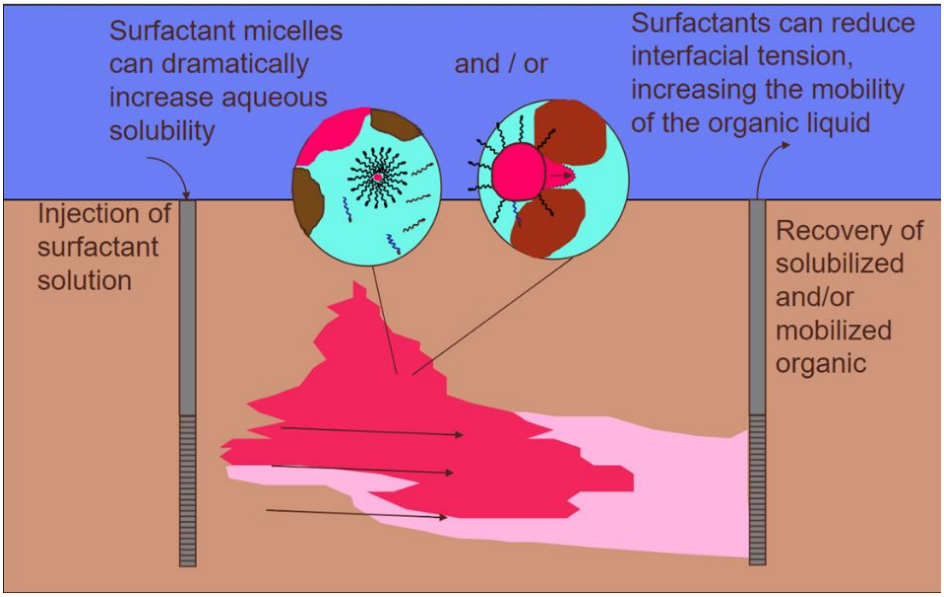

Figure.5. Mechanisms of Surfactant Flooding (Abriola, 2002)

Once injecting surfactant solution into the subsurface, surfactant micelles can increase the oil solubility in the aqueous phase and ideally reduce interfacial tension dramatically which will largely improve the mobility of the organic liquid. Then, we recover the organic phase from production wells, the separation process may be needed afterward to collect high purity crude or oily phase. In the illustration, red stands oil phase, light blue stands for aqueous phase, brown represents rock matrix and black dot symbols are surfactant molecules. Two primary mechanisms of this process are mobilization and solubilization (Nivas et al. 1996). The phenomenon of non-polar species partition into the organic interior of the micelles is called Solubilization (Nivas et al. 1996).

Hydrotrope

More than a century ago, Carl A. Neuberg found that by adding a particular type of compound can largely increase the solubility of the hydrophobic compound in water (Dhapte and Mehta 2015). These solubility-enhancing molecules were named hydrotropic agents or hydrotropes. Meanwhile, the phenomenon of this is called hydrotropy (Balasubramanian et al. 1989). There are some typical examples of hydrotropes such as sodium benzoate, salicylate, and xylene-sulfonate (Balasubramanian et al. 1989).

Hydrotropy may also be explained as a salting-in process; this idea has been pointed out by McKee, R. H in 1946. Hydrotropy can be an excellent example of the salting-in effect, which defined as in addition of certain salt compound will increase the charge of the solute molecule and lead to increasing the interaction with water molecule; then, improve the solubility in water.

Like surfactant, hydrotrope also contains the hydrophilic and hydrophobic part in their molecule, however; the major difference is hydrotropes have much smaller hydrophobic fraction so that there are too small to cause spontaneous self-aggregation (Nidhi et al. 2011). Nidhi and his group suggested that unlike the surfactant, hydrotropes do not have the CMC and do not form the aggregation that suddenly like surfactant, the process will be more gradual. Most hydrotropes even do not self-aggregate (Nidhi et al. 2011).

Phase behavior and HLD Equation

There are plenty of methods we can examine the phase behavior. Mathematical modeling and experimental method are most well-known methods to simulate the phase behavior under reservoir condition. To achieve the reservoir condition, we need to adjust the salinity, pH, temperature, pressure and additional parameters. To conduct the experimental phase behavior tests, a salinity scan of surfactant samples and HLD equation can be used to facilitate the formulation tasks and effort. The HLD equation for anionic surfactants is:

$$HLD = ln\ S - K(EACN) - f(A) + \sigma - a_T(DT) \quad (1)$$

Where,

S is the salinity in wt% NaCl (based on the aqueous phase)

K is a constant number depending on the type of surfactant head group *EACN* stands for the equivalent alkane carbon number, for instance, *EACN* of Decane is 10.

$f(A)$ is a function of the alcohol type and concentration

σ is a surfactant characteristic parameter, also known as Cc

a_T is the temperature constant, and DT is the temperature difference measured from the reference temperature (T_{ref} = 25 ◦C). (Witthayapanyanon et al. 2008; Salager et al. 1979).

$$\ln S^* = K(\mathrm{EACN}) - \sigma, \quad (2)$$

$$\ln S^*_{mix} = K_{mix}(\mathrm{EACN}) - \sigma_{mix}, \quad (3)$$

If the microemulsion is formed without the addition of alcohols (f (A) = 0) and at the

reference temperature (T = Tref = 25 ◦C), the general HLD equation listed in Eq. (1) can be simplified as shown in Eq. (2) and Eq. (3) (Witthayapanyanon et al. 2008; Salager et al. 1979) where Eq. (2) is for a single anionic surfactant system and Eq. (3) is for the mixed surfactant conditions. In the Eq. (3), an idealized linear mixing rule has been applied which gives the equation below. (Witthayapanyanon et al. 2008):

$$S^*_{mix} = S^*_i \quad (4)$$

$$\ln S^*_{mix} = \sum x_i \ln S^*_i \quad (5)$$

$$\sigma_{mix} = \sum x_i \sigma_i \quad (6)$$

$$K_{mix} = \sum x_i K_i \quad (7)$$

By examining the salinity of individual group of phase behavior samples, we can visually observe the optimal condition within the samples, and HLD value can be calculated to be zero value which means no deviation between the hydrophilic and lipophilic interaction energies (Witthayapanyanon et al. 2008). When the salinity of the sample reaches the optimum salinity situation, the surfactant system interacts equally with the oil and water phases and thus has the strongest affinity to accumulate at the oil-water interface; furthermore, resulting in formation of middle phase microemulsions with the minimum IFT and concomitant with highest oil solubilization (Witthayapanyanon et al. 2008). Results of negative, zero or positive HLD values suggest the formation of Winsor Type I, Type III or Type II microemulsions (Jin et al. 2017; Salager and Antón 1999). Salager and Antón also indicate that a positive sign means an increasing value of that variable would produce a Type I → Type III → Type II transition, while a negative sign would correspond to

the different transition (Salager and Antón 1999).

The microemulsion of phase behavior samples is explained in **Figure 6**. Salinity increasing from left to right and three different microemulsion types are observed with the perfectly matched IFT value on the bottom. Begin with the low salinity Type I samples on the left which is the "oil in water" microemulsion; then the Type III microemulsion reaches at a certain salinity while the interfacial tension becomes the lowest value (γ^*_{om}). In the end, the Type II microemulsion, "water in oil," is reached while increasing the salinity in the phase behavior samples. The typical “V” shape on the upper half or a "fish" shape in the whole figure is formed in the interfacial tension versus salinity plot.

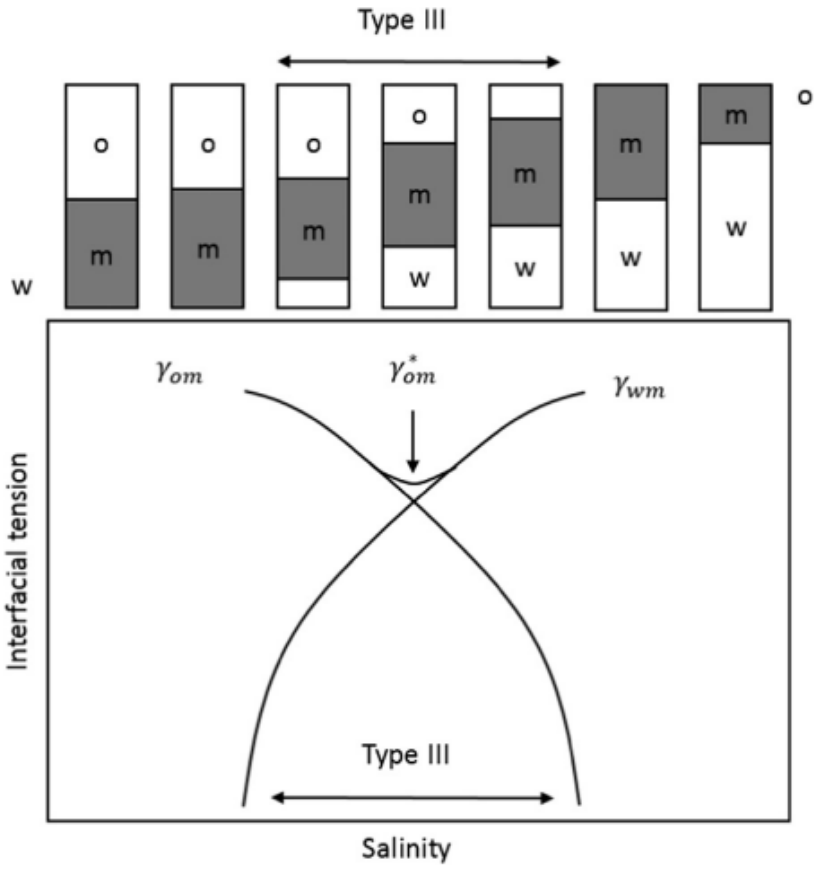

Figure. 6. Variation in interfacial tension versus water salinity (Jin et al. 2017)

Winsor R Ratio

To examine the phase behavior, in the early times, people also use Winsor R ratio approach, the classical equation of R ratio is listed below:

$$R = \frac{Aco}{Acw}$$

Where

A_{CO} is the cohesive energy per unit area between the surfactant and oil

A_{CW} is the cohesive energy per unit area between the surfactant and the water phase.

An R ratio less than one indicates Winsor Type I microemulsion which defined as the oil molecules go into the aqueous phase. R ratio higher than one represent Winsor Type II microemulsion which is the water molecules go into the oil phase, and an R ratio equal to unity indicates a bicontinuous microemulsion (type III or IV) where the surfactant-oil and surfactant-water interactions are identical (Bourrel and Schechter 1988). **Figure. 7** is an illustration adapted from the Handbook of microemulsion science and technology by Jean-Louis Salager and Raquel E Antón, which illustrates the relationship between R ratio and matched phase behavior observation.

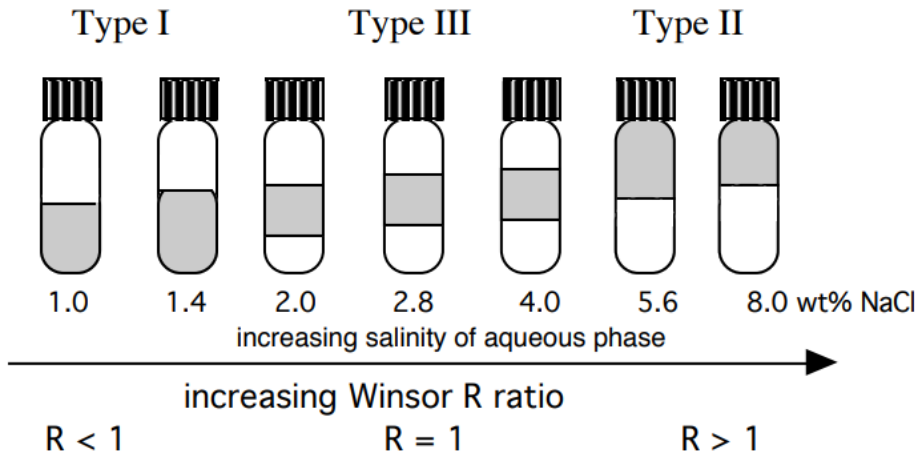

Figure.7. Illustration of R Ratio Corresponding to Typically Observed Phase Behavior (Salager and Antón 1999)

Surfactant Adsorption

Bera and few other people pointed out that the process of adsorption is the dissolved component separate from the solvent and transfer onto the surface of the adsorbent. According to the same group, this phenomenon is complicated due to the various potential causes such as reaction and mass transfer (Bera et al. 2013).

In the surfactant flooding system, adsorption occurs, surfactant adsorbed onto the surface of the rock and lost the effectiveness. One of the primary cause of this can be the surface charge of rock and interface of aqueous surfactant solution. The positively charged surfactants attract to the negatively charged rock surface, similarly; negatively charged surfactants will be captivated by the positively charged rock surface (Bera et al. 2013). There are some other significant parameters like pH and salinity are also play the considerable role of surfactant adsorption due to the ability to change the surface charge.

The study of adsorption is important, especially when applied to the surfactant flooding for Enhanced Oil Recovery (EOR) and surfactant enhanced aquifer remediation (SEAR) process. The adsorption study in the laboratory measurements of specific rock/sand corresponding to the reservoir fluid and condition is essential. It is helpful for obtaining more precise estimation of the reservoir environment; it can provide far better prediction of expenditure and amount of surfactant required at reservoir conditions.

III. Experimental

Materials

In this study, Heptane, Octane, Decane, and Dodecane are the pure alkanes being chosen as the oil phase, and properties of these hydrocarbons are displayed in **Table 1** below. These four types of hydrocarbon are from the same supplier, Sigma Aldrich. The purity of each one is, ≥ 99.5%, ≥ 98%, ≥ 95% and ≥ 99.5% in the order of increasing EACN. Sigma Aldrich also provides sodium chloride (NaCl) used in the phase behavior study, and the effective weight percentage is above 99%.

Table. 1 Properties of Four types of Pure Alkane Hydrocarbon

Name	Chemical Formula	EACN	Density, g/ml	Molecular weight, g/mol
Heptane	C_7H_{16}	7	0.684	100
Octane	C_8H_{18}	8	0.703	114
Decane	$C_{10}H_{22}$	10	0.73	142
Dodecane	$C_{12}H_{26}$	12	0.75	170

As discussed in the previous introduction section, there are two surfactants is chosen in this study. They are 0.75% dioctyl sodium sulfosuccinate (AOT) and 0.19% sodium dodecyl benzene sulfonate (SDBS) by weight percentage. Dioctyl sodium sulfosuccinate, AOT, is from a supplier Sigma-Aldrich and it is white waxy chemical

which has more than 97% active. SDBS is from Sigma Aldrich as well with a 79.7% activity.

Urea and Sodium Xylene Sulfonate are selected as hydrotropes in this study. The supplier is also Sigma-Aldrich, and it's 99% and 91% active by weight percentage. The first reason for choosing urea is the low cost and high safety features. People even put urea into the makeup and skincare products. The second reason is that urea as a hydrotrope; it is also an optimizing CO_2 generating agent (Wang et al. 2018). Wang and his colleagues have accomplished this new application in the past few years. Urea can be used in the in-situ CO_2 generation for enhanced oil recovery (Wang et al. 2018). To choose urea as the hydrotrope, we may benefit from it more than just a simple role of hydrotrope due to the CO_2 generation under proper conditions. As for comparison purpose, another common hydrotrope, sodium xylene sulfonate (NaXS), is chosen. It is found in personal care products, primarily in shampoos, because of its ability to serve as a claritant or wetting agent that helps a formula spread more easily and ensure efficient cleansing (Johnson 2018).

Methods

A series of methods and tools were used to cover different aspects of the aim in this study. First, the phase behavior test. The 14mL glass vials are chosen which contain 5mL surfactant solution mixing with 5mL hydrocarbon. Coalescence rate is the time spend to form clear type III emulsion after manually shacking of the vials. Interfacial tension was measured using a spinning drop tensiometer; the rotating speed is set to

approximately 4000 rpm. The adsorption test is done by preparing SDBS solutions in seven different concentrations and mixing with selected porous media for 72-hr equilibrium time. The adsorption amount is calculated by comparing the concentration of SDBS in the supernatant after the mixing and before 72-hr adsorption.

Phase behavior Study

Phase behavior study is the visual observation of the surfactant system behavior by mixing the equal amount of aqueous phase and oil phase. In this study, a 5ml of surfactant solution with DI water which can be described as the aqueous phase and mix it with 5ml of selected hydrocarbons from Table 1. First, the aqueous phase is added into the 14ml flat bottom glass tube, and then a line of aqueous phase level is marked on the glass tube using a color marker. Then the oil phase is added into the test tube and wrapped with Teflon tape on the opening to control the volatilization and loss of solution. This marked line is a quick and straightforward approach to compare the location of the aqueous phase before and after adding the oil. It conveniently points to the right type of microemulsions formed. If the marked line is below the interface of the oil and water, aqueous phase enlarged which it is an oil in water solution. Then, it is defined as the Winsor Type I microemulsion. Otherwise, if the marked line is beyond the interface of oil and water, it means the water is going into the oil phase; thus, it is going to be Winsor Type II microemulsion. If there is a middle phase between the oil and water, it is Winsor Type III microemulsion. After three-day equilibration period, the photos of the samples were taken, and the resulted microemulsions and types were recorded.

Coalescence rate

Coalescence rate is visually observed in type III microemulsions. It is measured after samples are manually flipped 3 to 4 times. The coalescence rate is defined as the time needed when the oil-microemulsion and water-microemulsion boundaries were sharply formed even if the excess oil or water is still opaque. Sometimes, faster coalescence does not mean better system; as long as the coalescence rate is less than 15 minutes, the results of better formulations are acceptable. The targeted coalescence rate can be different depending on the actual circumstances and oil properties (e.g., long-chain or multicomponent molecules).

Interfacial Tension

A spinning drop tensiometer is applied in this interfacial tension measurement. A capillary glass tube and a syringe were also used to hold the aqueous phase for the injection of the oil phase. First, fill the capillary tube with an aqueous phase from the bottom of phase behavior samples. During this process, it should not introduce any bubble in the capillary tube; otherwise, the bubble will influence the measurement and cause the error. Then insert the tube into the tensiometer horizontally. Afterward, approximately 2 μL of the oil phase is carefully injected into the center of the capillary tube by the glass syringe. For each IFT measurements, the aqueous phase and oil phase need to be acquired from the matched samples from the phase behavior study. Then, the rotation speed of tensiometer is set to approximately 4000 RPM, and oil droplet requires to be maintained in the center of the test tube without movement, and no contact of the ends on both sides. Record the diameter reading of the oil droplet every

5 minutes with the actual rotational speed until the change of the reading is less than 5% change compared to the previous reading. All the recorded data need to be inserted into the excel file, and interfacial tension will be calculated in a unit of mN/m.

Adsorption Test

First, prepare seven different concentrations of SDBS surfactant solution from 300 ppm to 1500 ppm, 10 grams of each in the 40 ml test tube separately. Then, mixing the 10 grams of surfactant solution with selected sand/soil for 72-hr equilibrium time. Samples are manually flipped every 12 hours. After equilibration, samples are centrifuged and filtered to remove suspended clays and other fine particles before analyzing the concentration of surfactant in the supernatant by UV-Vis. Three types of media were tested in this study. They are Ottawa sand, Indiana limestone, and activated carbon. With the fixed amount of surfactant solution, the solid amount is different based on the adsorption ability. The amount of porous media used in this study of Ottawa sand, Indiana limestone, and activated carbon are 5 gram, 3 gram, and 0.5 gram, based on considering their capacity of surfactant adsorption and residual surfactant levels in the treated solution being able to quantify. The adsorption amount is calculated from the milligram of surfactant adsorbed divided by the actual amount of sand in the unit of the gram.

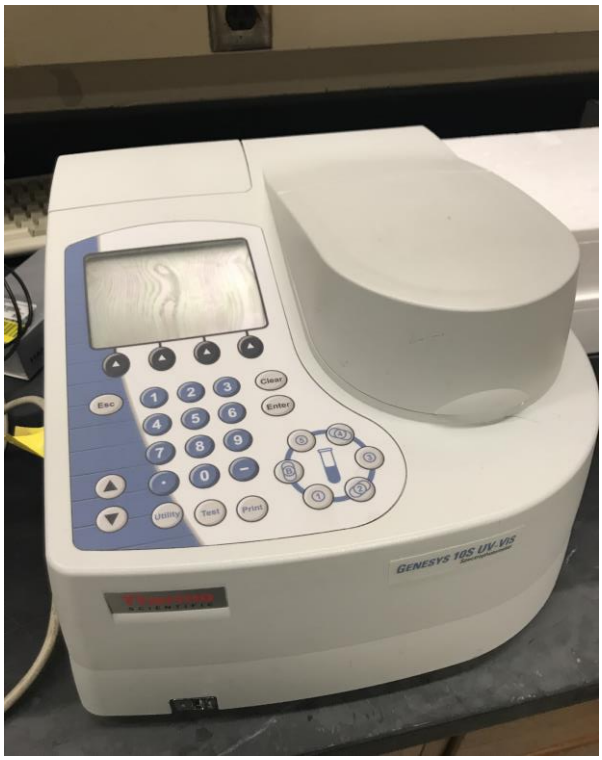

Figure 8. Thermo Scientific: Genesys 10s UV-VIS Spectrophotometer

A new method of using UV-vis to measure the SDBS concentration is set up to measure supernatant after adsorption. The baseline is the DI water, and the scanning wavelength is in the range of 190-300 nm. UV-Vis Spectrophotometer is a measure the absorbance which is the amount of light absorbed by the solution shown in **Figure 8**. Calibration is created since there is an apparent linear relationship between the SDBS concentration and absorbance as shown in **Figure 9** below. As we can see from the figure, Case one is the surfactant with DI water case and Case two is the surfactant with urea added case.

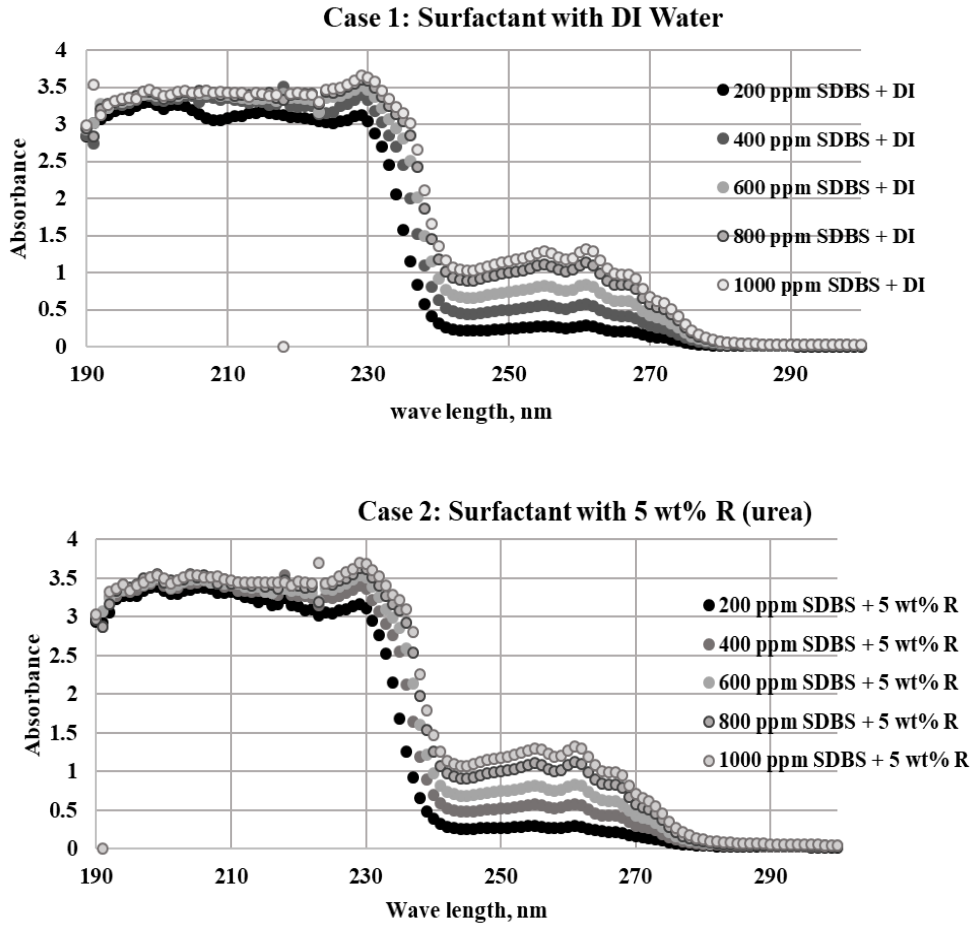

Figure. 9. Calibration of Absorbance for SDBS only (top) and SDBS with 5% Urea (bottom) on 190 to 300 nm Wavelength.

Calibration curves are developed for both surfactant-only formulations and surfactant with hydrotropes mixtures. The selected wavelength is 262nm. It can be seen in the graph above, from 190 to 240nm, the absorbance responses are exceeding the reasonable upper limit (> 2.0) and not reliable. The response around 260 nm is representative, and 262 nm is selected wavelength which is the peak in the figure.

The various concentration of urea with SDBS 1000 ppm solutions are also tested, urea reading showed no impact on SDBS reading at the selected wavelength. During the

adsorption test, SDBS is the primary surfactant analyzed in this study. As for sodium xylene sulfonate, the calibration curve and impact on SDBS responses is also examined.

Surface Tension Measurement

Attension® Theta is an advanced and versatile contact angle meter for highly accurate measurements of static and dynamic contact angle and surface and interfacial tension (Biolin Scientific). The experimental apparatus is shown in the **Figure 10** below. A computer with the software is connected to the equipment for the real-time analyzation. A syringe needle, a pump, and the pipeline are connected for injecting the fluid. After the pendant drop formed, the shape of a droplet is analyzed by the software shows in **Figure. 11**. The surface tension of the pendant drop in the air is calculated and recorded.

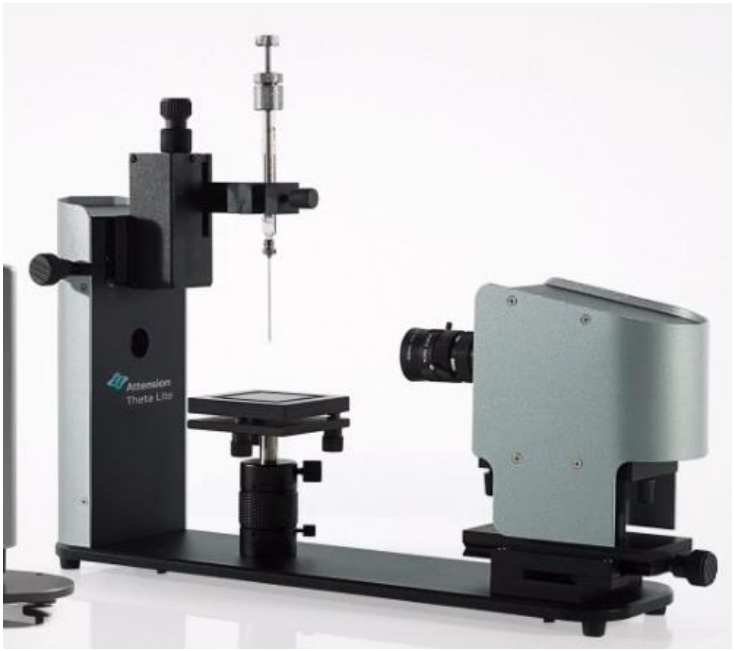

Figure. 10. Attension Theta Optical Tensiometer (Biolin Scientific)

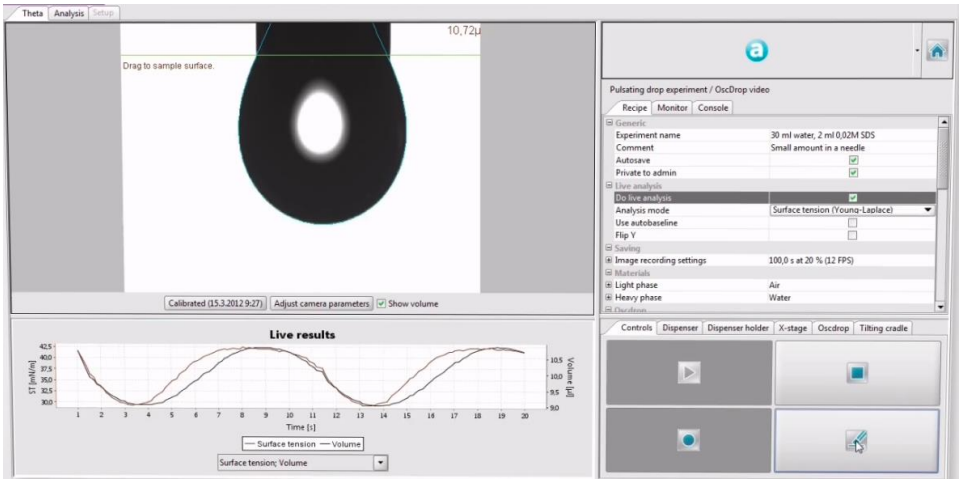

Figure. 11. Attension Theta Optical Tensiometer Operation Software (Biolin Scientific)

Stability test

Stability test of the aqueous solution is also carried out to examine the surfactant solution stability. For the surfactant only case, the 5 ml surfactant solutions are prepared in the 15ml flat bottom test tube which contains 0.75% AOT, 0.19% SDBS and DI water by weight percentage. For the surfactant with hydrotrope cases, an addition of 5% urea and 1% NaXS samples also tested for comparison requirement. Samples with selected salinity range are provided and set on the laboratory bench. Changes in the solution are recorded daily up until the end of 2 weeks period.

IV. Results & Discussions

Phase behavior of Case I (Surfactant Only without hydrotrope)

The case I system contains surfactant-only with DI water. The surfactant solution contains 0.75% AOT and 0.19% SDBS by weight percentage. The numbers on top of each phase behavior samples represent the NaCl salinity scan. Blue color stands for type I microemulsion, red is type III, and green stands for type II microemulsion. The color lines on the test vials are marked before adding the oil phase as mentioned in the previous section. It's a tool to diagnose whether it is an oil in water or a water in oil microemulsion.

Phase behavior samples are shown in the figures below from **Figure. 12** to **Figure. 15**. Figure 12 is the surfactant with Heptane samples. The Winsor Type III window is narrow that only one sample is observed (salinity of 0.7%). **Figure 13** is the phase behavior samples contains the Octane as the oil phase. The type III window is also really narrow which means it is salinity sensitive since only the salinity of 0.9% sample gives the Type III microemulsion. In this sample, the water-microemulsion and the oil-microemulsion boundary are evident compared to heptane samples.

0.4% 0.6% 0.7% 0.8% 1.0%

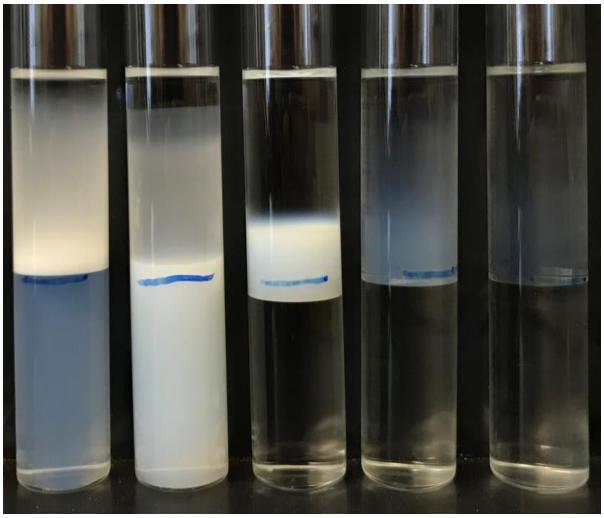

Figure 12: Salinity scan for Case 1 with heptane

0.8% 0.9% 1.0% 1.2% 1.4%

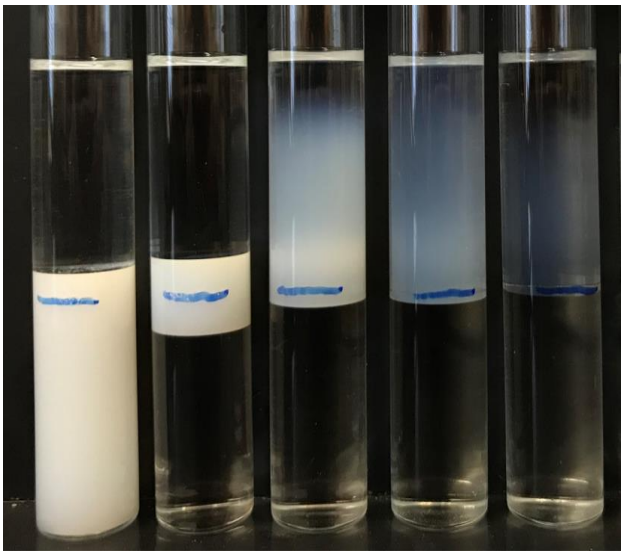

Figure 13: Salinity scan for Case 1 with Octane.

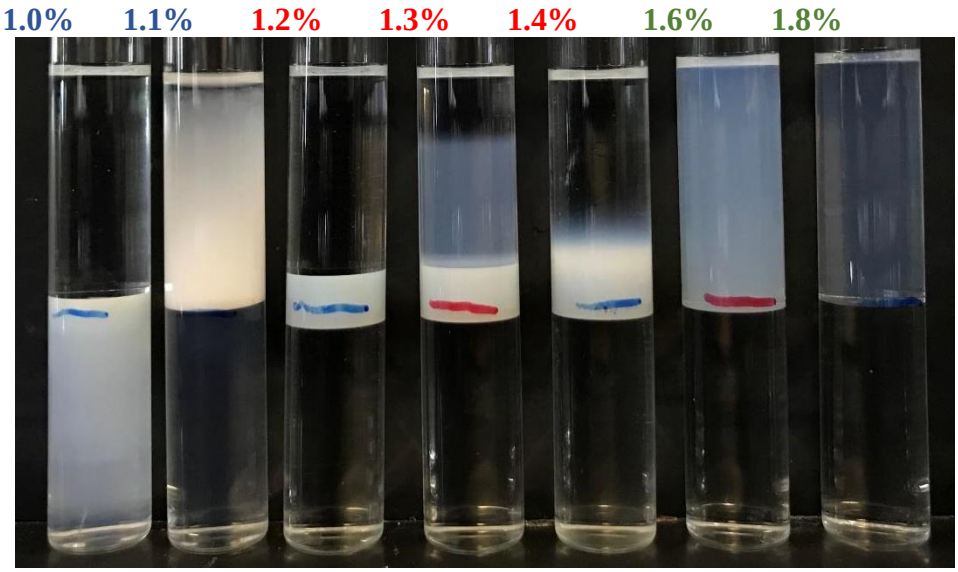

Figure 14: Salinity scan for Case 1 with Decane.

Phase behavior samples which contain decane and dodecane are shown in **Figures. 14** and 15. Decane samples provide a wider type III microemulsion range compare with previous two sets of samples. Decane samples shown in the photo can produce 3 different salinity concentrations with type III microemulsion. However, when doing the same NaCl salinity scan for dodecane, only two samples exhibit a clear type III microemulsion. The middle phase is quite thinner to detect and apparently has mcuh higher viscosity.

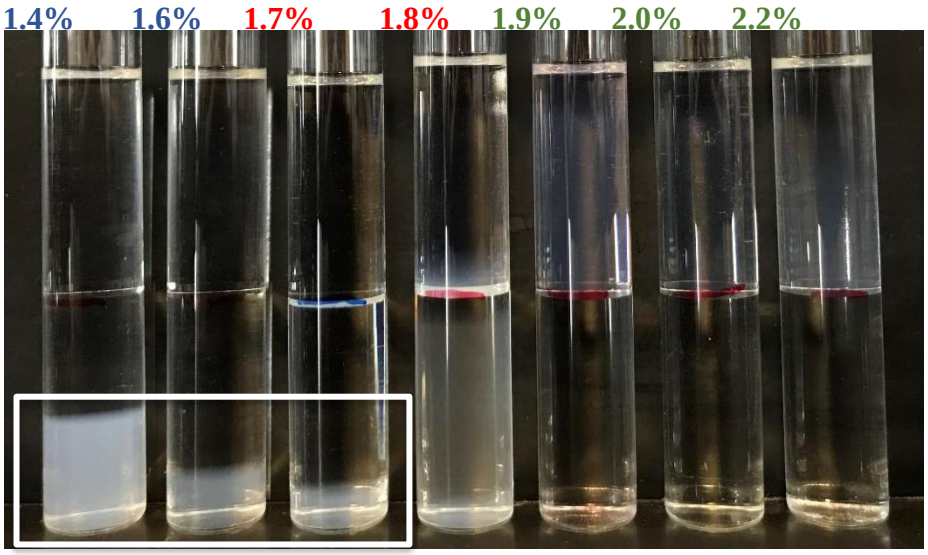

Figure 15: Salinity scan for Case 1 with Dodecane.

There is a critical observation that the dodecane samples shown in Figure 15 did phase separate only one-day long which was denoted inside the white line. This SDBS and AOT formulation are not stable when mixing with dodecane in lower salinity concentration range.

Due to the phase separation issue, stability rest is needed to determine how the surfactant solubilizes in the aqueous phase and how long it is stable after mixing with water but before add oil phase. Stability tests results are shown in the later section.

Figure.16 is the optimum salinity point based on IFT measurements as a function of equivalent alkane carbon number (EACN). The linear relationship is observed from the graph. The Winsor Type III window is shown in **Figure.17**. Symbols of square dots represent type III samples; rhombic dots are type I samples and rounded ones represents type II samples. It is evident that the type III range is limited and salinity sensitive, only changing 0.1 % of salinity results in distinct types of the microemulsion.

Figure.18 is the Interfacial tension measurements of four types of hydrocarbon for comparison. The IFT less than 0.01 is consider the ultra-low IFT which is also related to type III microemulsion. The sharp V shape can be seen from the graph and matches the literature graph.

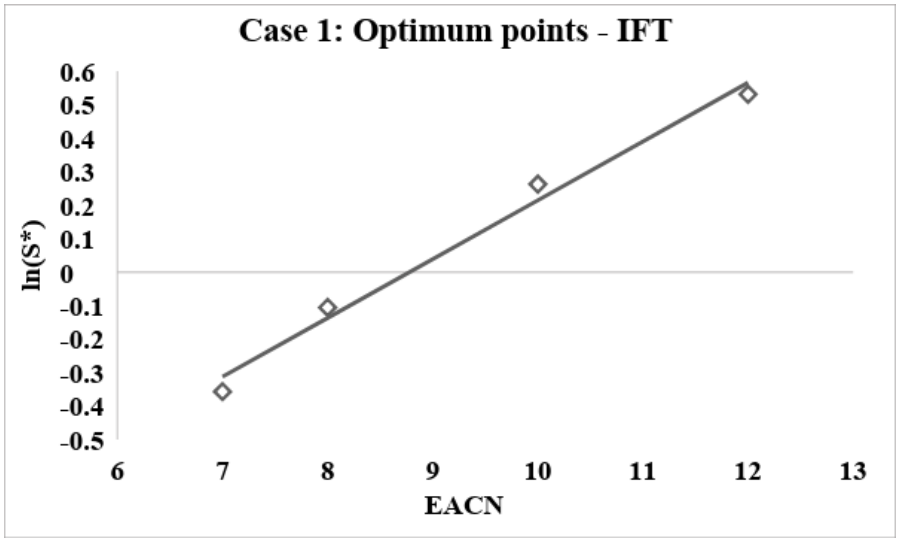

Figure 16. Natural log of salinity vs. EACN for Case 1(Surfactant with DI Water) optimum points

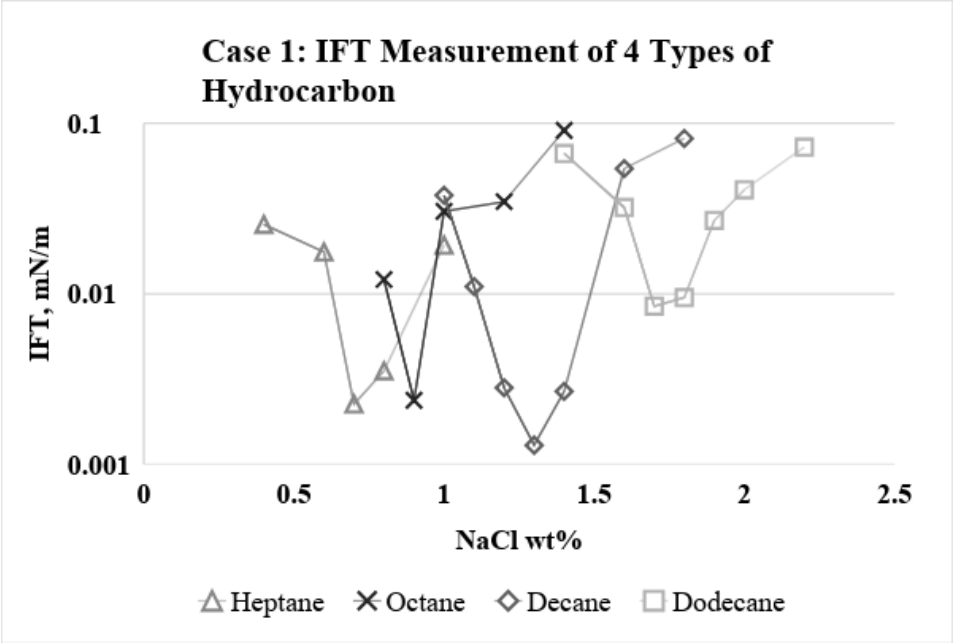

Figure 17: IFT vs. salinity for Case 1(Surfactant with DI Water)

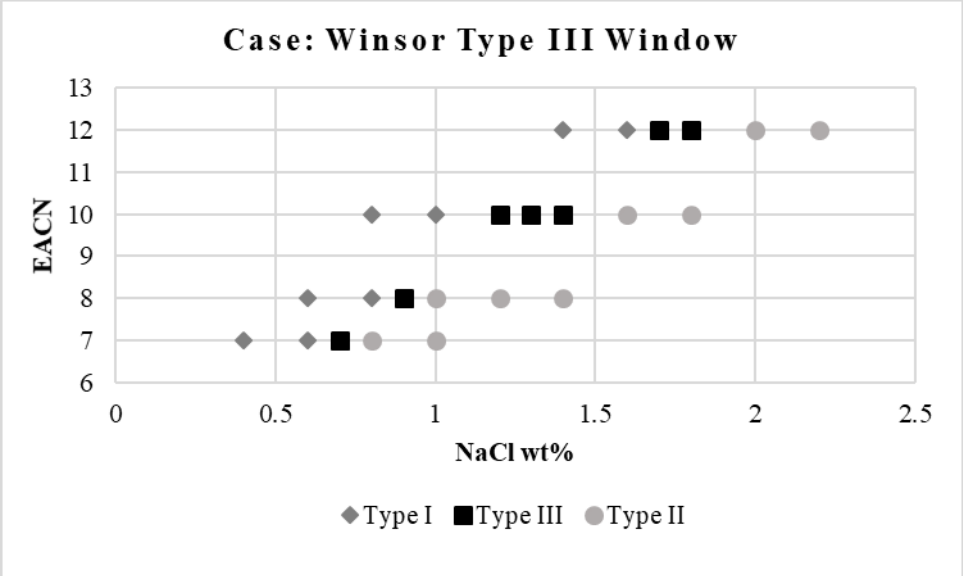

Figure 18: EACN vs. Salinity for Case 1 with microemulsion type identified

Phase behavior of Case II (Surfactant with 5% Urea)

Case 2 is the Surfactant with hydrocarbon samples and urea of 5% added. Phase behavior samples with different oil phase are shown from **Figures 19** to **Figure 22**. When compare with surfactant-only case, type III window becomes more broaden, and the resulting middle phase becomes more transparent in color. A wider Type III range allows operators a more accessible and convenient operation environment. If the surfactant formulation being used on a field site, a wider range of salinity is especially easy to handle in the field. Also, an increased optimum salinity, as well as the improved coalescent rate, is given potential to the higher salinity tolerance. For the stability issue mentioned in Case 1 with Dodecane as the oil phase, it is being optimized; no more phase separation issue after two weeks.

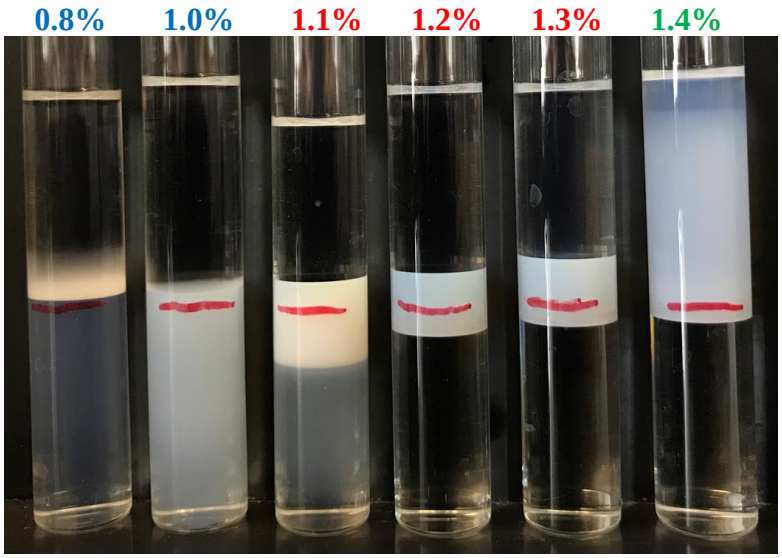

Figure 19: Salinity scan for Case 2 with heptane.

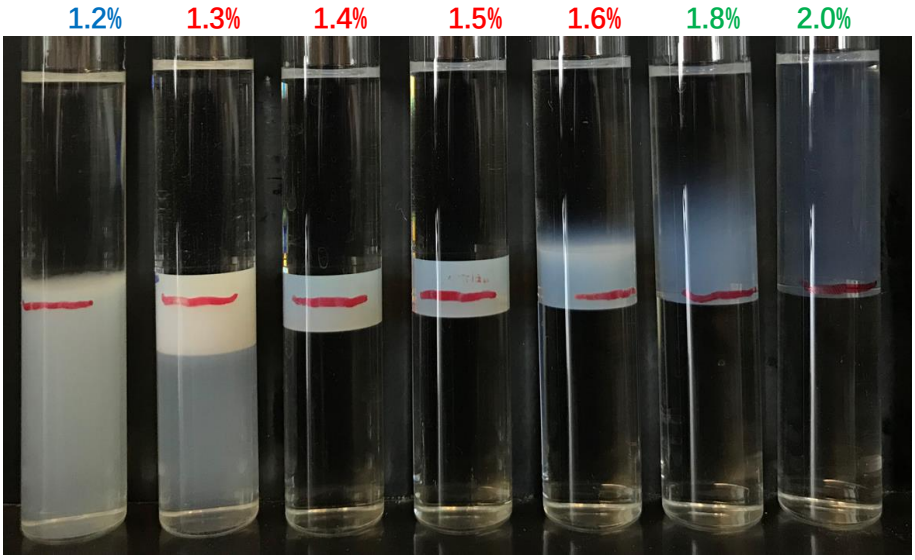

Figure 20: Salinity scan for Case 2 with Octane.

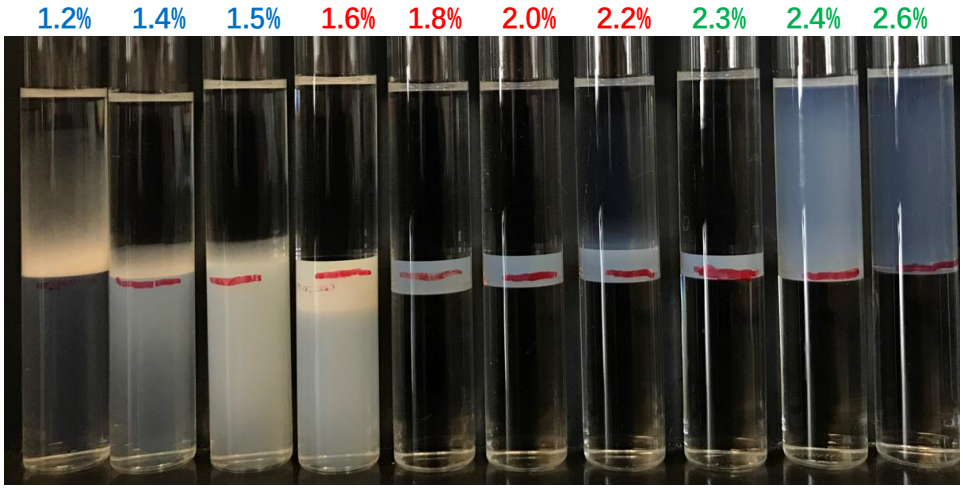

Figure 21: Salinity scan for Case 2 with Decane.

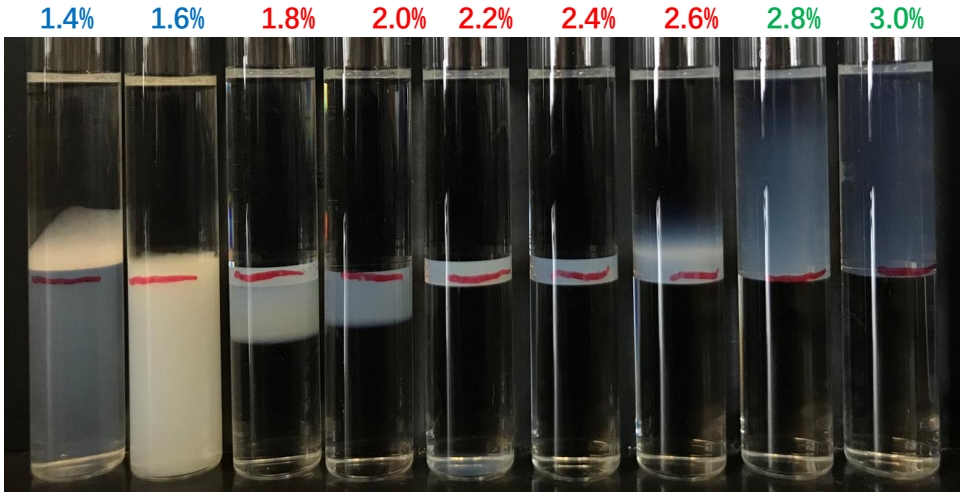

Figure 22: Salinity scan for Case 2 with Dodecane.

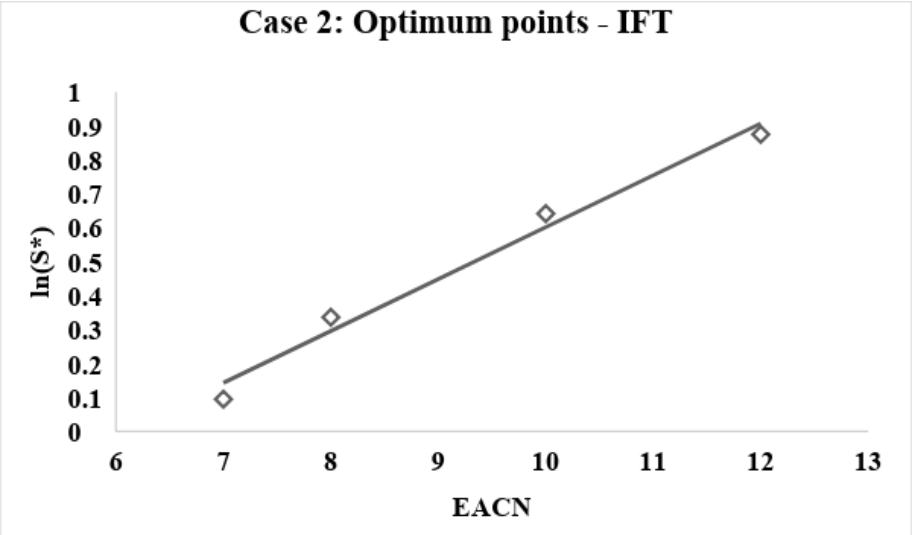

Figure 23. Natural log of salinity vs. EACN for Case 2 optimum points

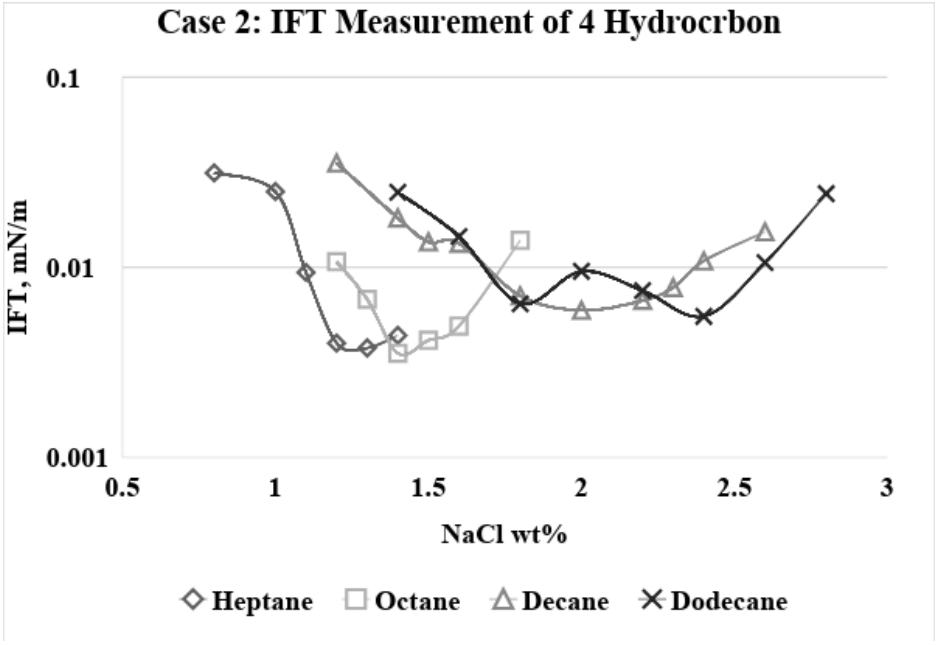

Figure 24: IFT vs. salinity for Case 2.

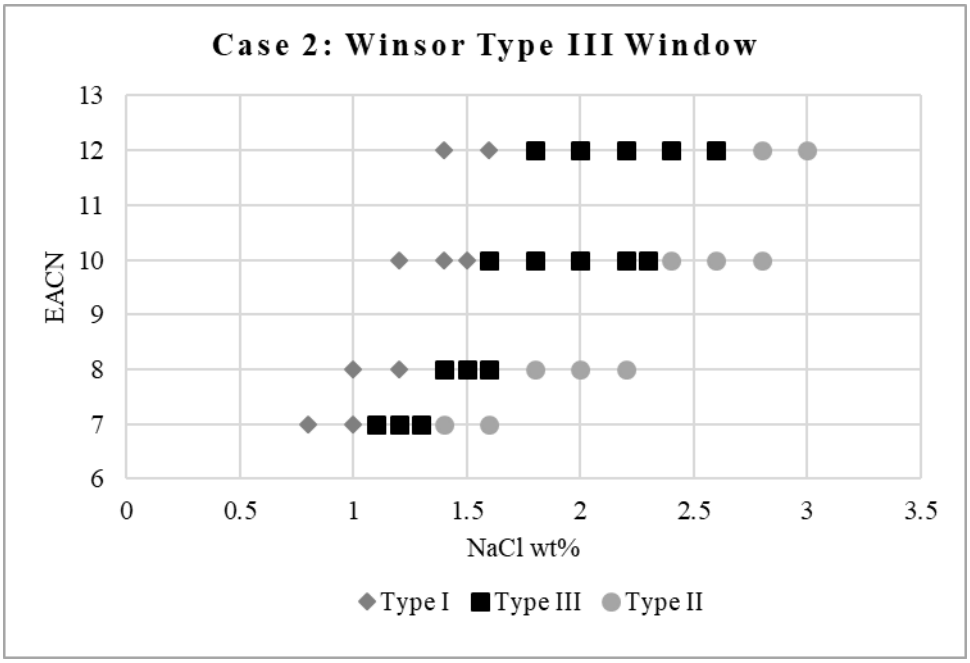

Figure 25: EACN vs. Salinity for Case 2 with microemulsion type

Figure 23 is the optimum salinity point based on IFT measurements as a function of equivalent alkane carbon number. The linear relationship is evident observed from the graph. The K and Cc number can be obtained. The Winsor Type III window is shown in **Figure 25**. Again, the square, rhombic and rounded dots represent type III, type I and type II microemulsions. Type III window is much wider to be observed compared to Case 1 which means it is less salinity sensitive. Heptane and octane, in this case, has 0.3% salinity fluctuate range within type III microemulsion, while decane and dodecane have 0.5% salinity fluctuate range within Type III microemulsion. Changing 0.1 % of salinity, may not result in microemulsion type change. **Figure 24** is the Interfacial tension measurements in the log scale of four types of hydrocarbon for comparison. Again, the interfacial tension at 0.001mN/m is considered to be the ultra-low IFT which represents Type III microemulsion. Moreover, the V shape can also be seen from the graph, but when compared to Case 1, the curve is much flatter shape which mean more Type III microemulsion is observed.

Phase behavior of Case 3 (Surfactant with Sodium xylene sulfonate)

Sodium xylene sulfonate is chosen as the second tested hydrotrope. Case 3 is the surfactant (AOT and SDBS) with hydrocarbon samples, 5%, 1% and 0.5% sodium xylene sulfonate (NaXS) added. Phase behavior samples with different heptane and dodecane as the oil phase are shown starts in **Figure 26**. The various concentrations of NaXS have been examined and present below. The 5% NaXS concentration has been tested first to be identical with the 5% urea added case. The salinity(NaCl)

weight percentage is on the top of the matched samples.

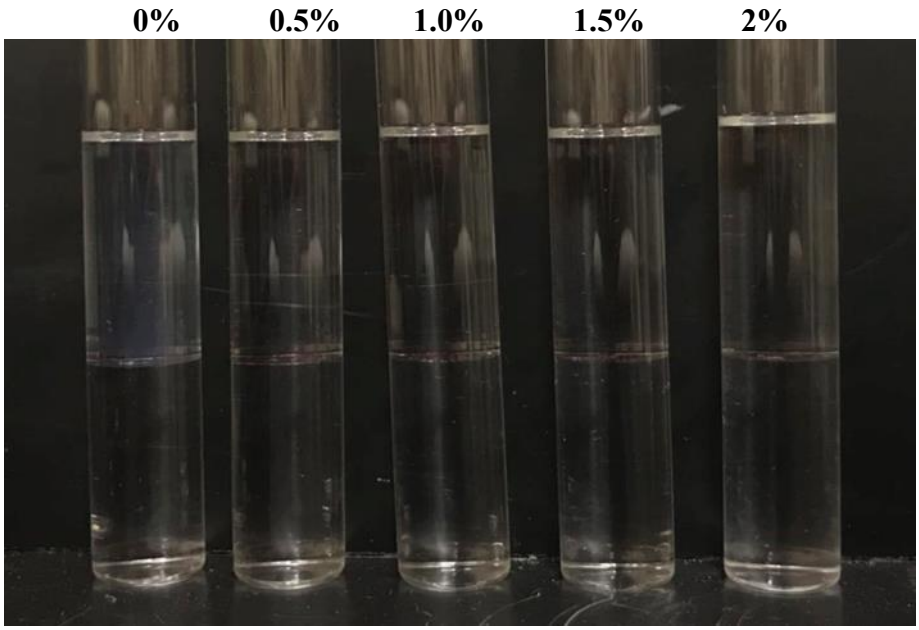

Figure. 26: Salinity scan for 5% NaXS with Heptane at room temperature.

As seen from the figure above, it is all clear type II from left to right which is ranging from no NaCl condition up to 2% NaCl. There are two reasons for this phenomenon: it can be NaXS introduce salt into the system, makes the current system at the higher salinity range which lies in the type II range. Another reason may be the NaXS itself contribute to the hydrophobicity of the solution, which makes the system more hydrophobic and shifts the optimum salinity to the lower salinity range. Thus, the samples are heated in the 50°C oven for 4 hours (**Figure 27**). Then the photos were taken, and the results are compared.

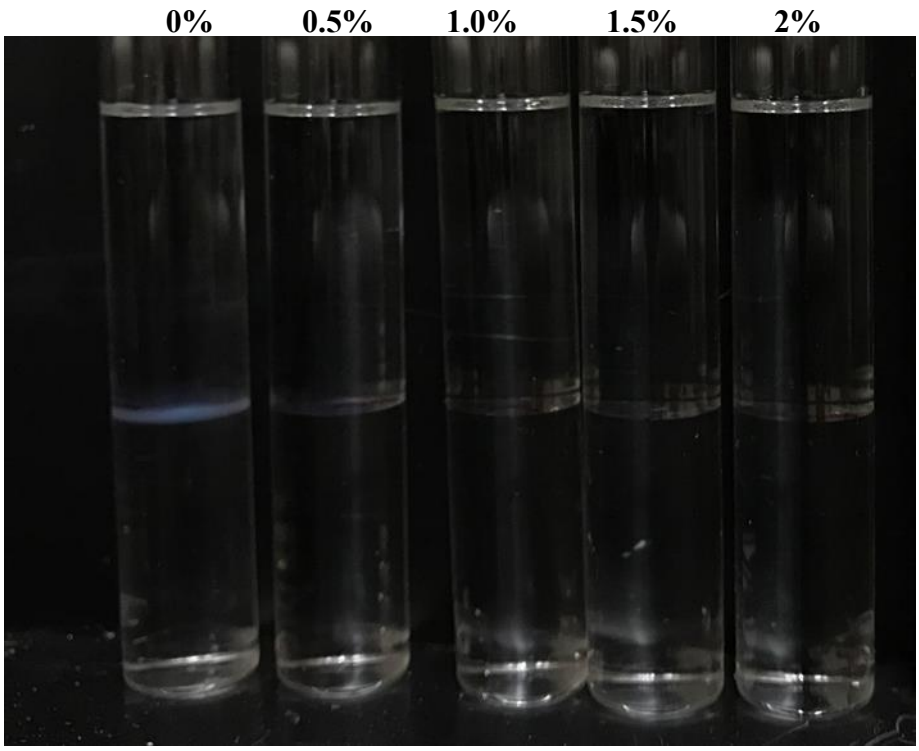

Figure 27: Salinity scan for 5% NaXS with Heptane at 50°C.

When compared with the room temperature samples, it is evident that the samples at zero salinity show a thin middle phase. According to HLD equation, increased temperature will increase the hydrophilicity of the whole solution, which is clearly matching the data observed. After increasing temperature, the optimum salinity of the solutions shifts to the right and appear in the photo above.

To examine another reason, NaXS introducing salt, the concentration of NaXS is decreased from 5% to 1% and redo salinity scan. It may be too much cations introduced to the system with additional 5% NaXS. If fewer NaXS in the system, a type III sample may appear in the selected salinity range. The result is shown in **Figure 28** below. The salinity of each sample is matched above them.

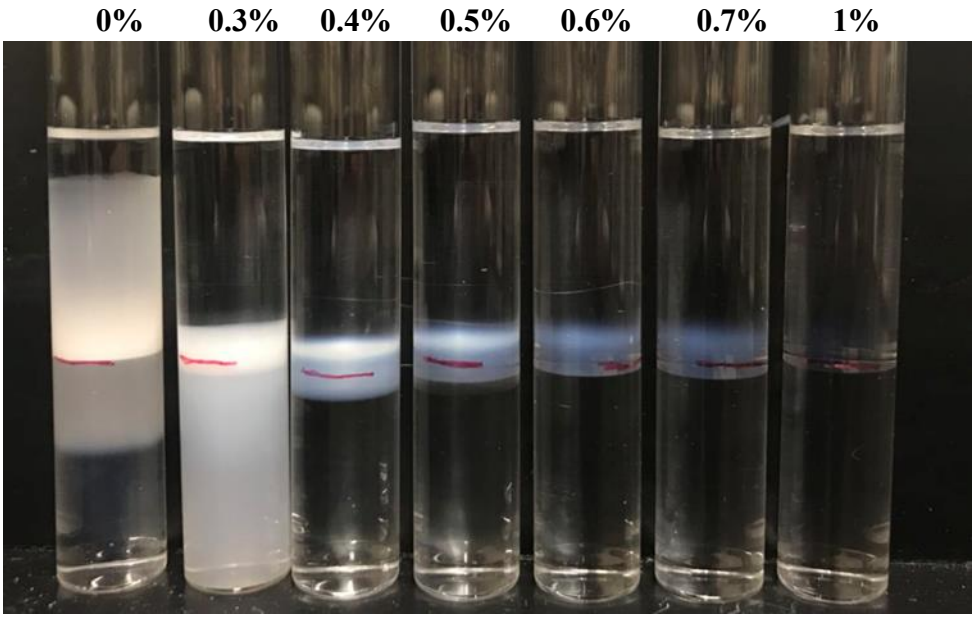

Figure 28. Salinity scan for 1% NaXS with Heptane at room temperature.

By reducing the concentration of NaXS, the type III microemulsion range shifts. Compare with 5% NaXS added case, an addition of 1% NaXS is clear to observe all different types of microemulsions. No salinity sample forms a gelation phase in the oil phase which makes the sample looks unusual. The gelation is considered the hydrogel which is not a strong gel formation. The sample with 1% NaXS shows a broader range of type III microemulsion; however, NaXS shifts the optimum salinity to the lower concentration.

It is obvious that the middle phase looks even more transparent compared to the previous two cases. A decreased optimum salinity, as well as improved coalescent rate, increases the potential of this surfactant system to work for the low salinity site. For instance, in the groundwater remediation process, a low salinity or no salinity injection fluid is required because of the environmental concern from the state's law or other ordinances. This is also the reason people introduce $CaCl_2$ into the surfactant

system to replace the high NaCl concentration since the efficiency for $CaCl_2$ is higher than NaCl.

Heating the sample to 50°C for 4 hours also contribute to the transparency of the middle phase shown in **Figure 29** below. Besides, the gelation in the zero-salinity sample did not break up to 50°C. The cloudy line between the oil phase and middle phase is thinner in the salinity of 0.3% to 0.5% samples, on the contrary, the opaque line formed between the middle phase and bottom aqueous phase with NaCl concentration greater than 0.6% and above samples. This cloudy line is also a symbol of surfactant lactation in this water in oil microemulsion. The enlarged image of 0.6% salinity sample is present in **Figure. 30** for clear observation.

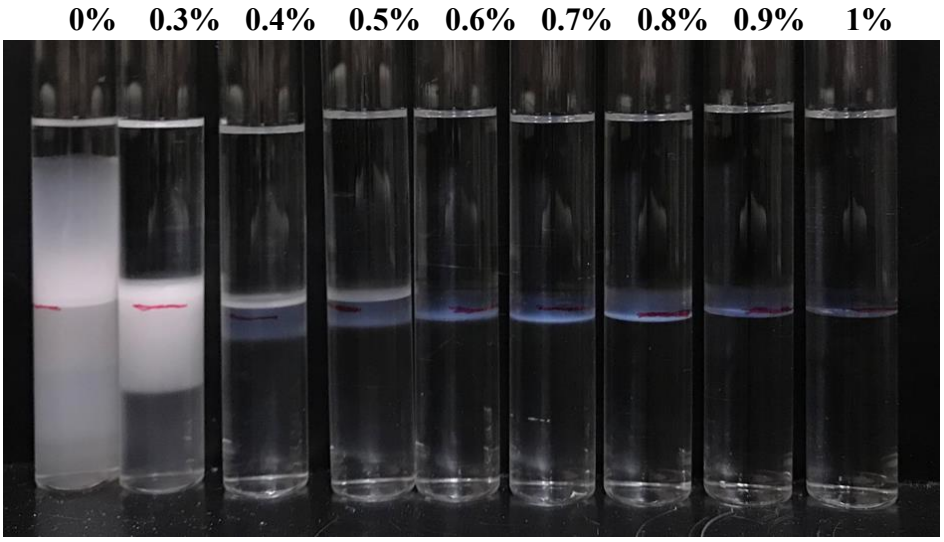

Figure 29: Salinity scan for 1% NaXS with Heptane at 50°C.

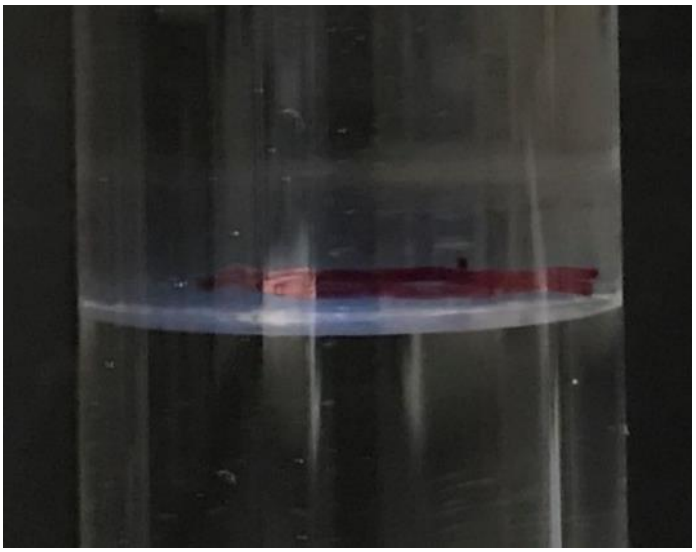

Figure. 30: Middle Phase of Surfactant Sample contains 1% NaXS, 0.6% NaCl and Heptane at 50°C.

Moreover, the addition of 0.5% NaXS with the surfactant system is also tested (**Figure.31**). There is no significant difference at this point. Type III microemulsion and middle phase appearance all looks similar with the 1% NaXS case. The optimum salinity increased 0.2 wt% from 0.4% to 0.6% when compared to the 1% NaXS added case. But, still slightly decrease the optimum salinity of the whole surfactant solution. The phase behavior result is in the figure below; the upper image is taken at the room temperature while the lower picture is taken after 4 hours heating in a 50°C oven.

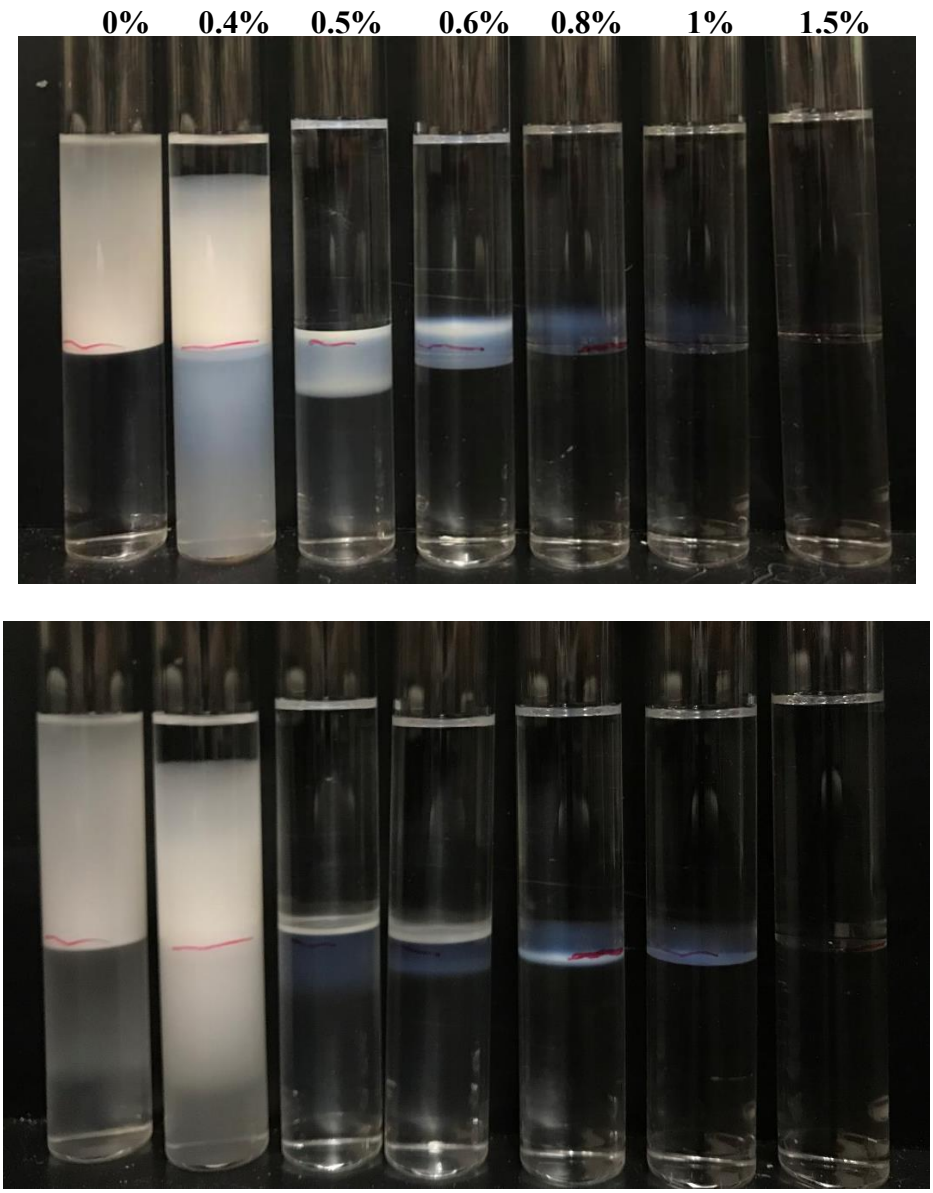

Figure. 31: Salinity scan for 0.5wt% NaXS with Heptane at Room Temperature (upper) and 50°C(lower).

A critical improvement of adding urea into the surfactant system is to solve the phase separation issue in the low salinity range with heavier oil(dodecane). Thus, the 1 wt% NaXS addition with dodecane is also tested to check if NaXS also contribute to the stability of the surfactant solution. The result is shown in **Figure 32**.

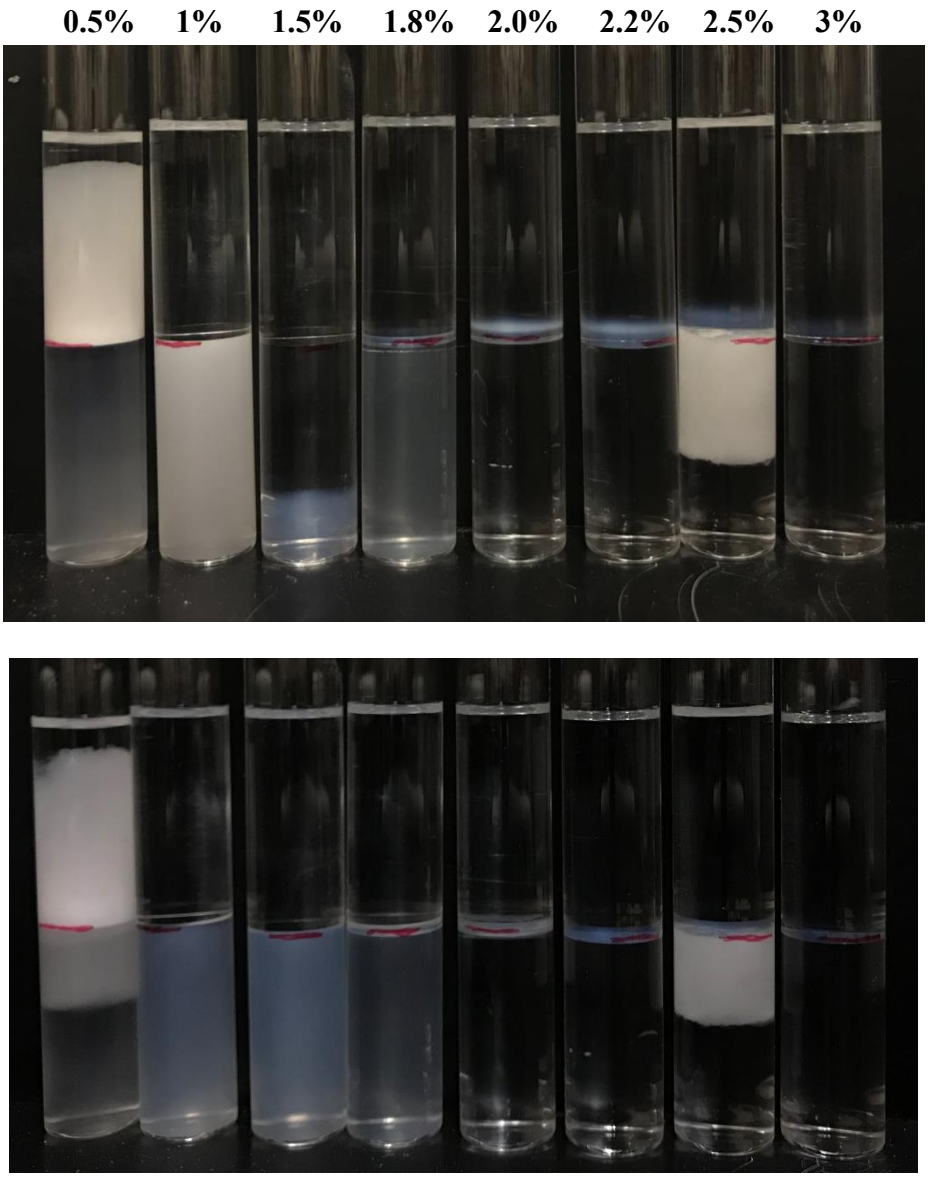

Figure.32: Salinity scan for 0.1wt% NaXS with Dodecane at Room Temperature (upper) and 50°C(lower).

Unfortunately, when mixing with dodecane, there is one sample at 1.5% NaCl has the phase separation issue again. However, for the type III range, it is improved to be more extensive, from 1.8% to 2.2%, but the optimum salinity is not shift much; still similar with the surfactant only case. When heating the samples to 50°C, the phase separation issue is solved.

Stability Test

To examine the phase separation issue and aqueous phase stability. In **Figure 33**, a set of stability test samples is prepared.

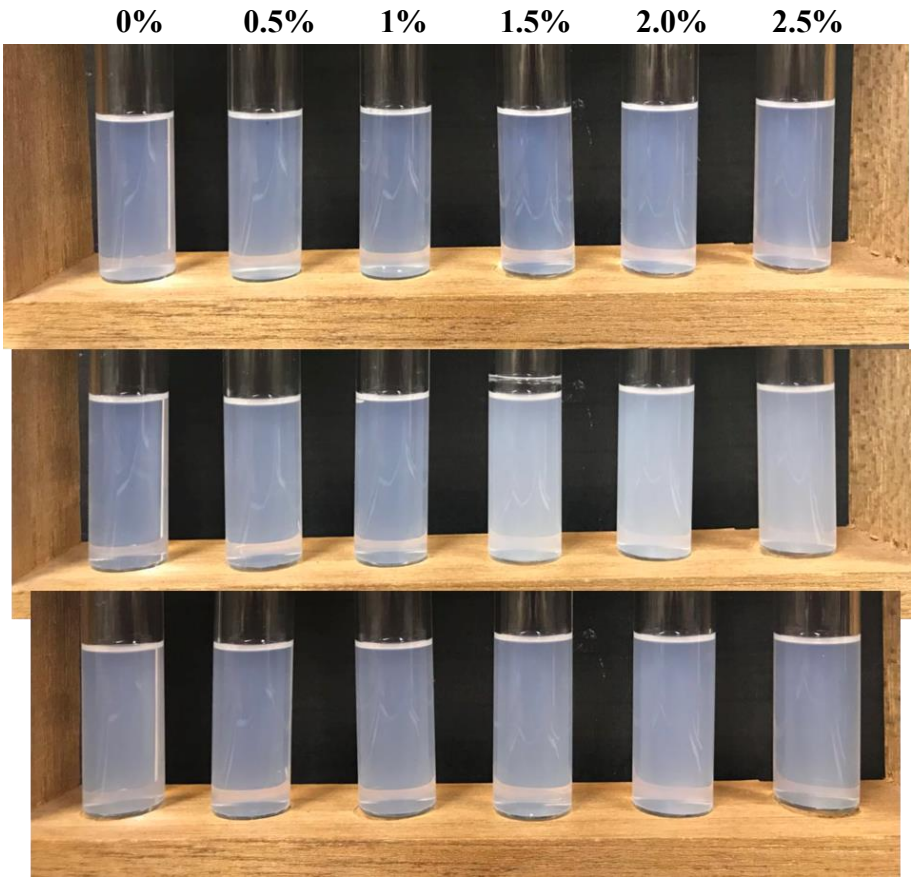

Figure.33. Stability Test Samples with 0.75% AOT, 0.19% SDBS and NaCl. Surfactant only (top), with 5% urea (middle) and 1% NaXS (bottom).

These 5ml stability test samples contain two surfactants (0.75 wt% AOT and 0.19 wt% SDBS), two types of hydrotrope and NaCl. The salinity of each sample is marked on top of them. The top 6 samples are surfactant with DI water; samples in the middle are the surfactant with 5% urea, and bottom set of samples are surfactant with 1% NaXS.

The photo is taken after two-day of equilibrium time. These samples are stable and no precipitation up to 6 days. Then the higher salinity (more than 1.0% salt) samples will have a minute amount of cloudy phase on the bottom of the test tube display in **Figure.34**. The dioctyl sodium sulfosuccinate (AOT) has a complicated phase behavior. Although the AOT used is more than 97 wt% purity, it still generates some complex phenomenon. This precipitation may due to the self-aggregation of AOT micelles along with time. This phenomenon is also viewed in the AOT stock solution. When first prepare the 1% stock solution of AOT and DI water, the solution is transparent within a week; however, as time goes by, the AOT solution will generate some white precipitation on the bottom of the tube and bring cloudiness to the solution. It should be the large aggregation of micelles settle down on the bottom.

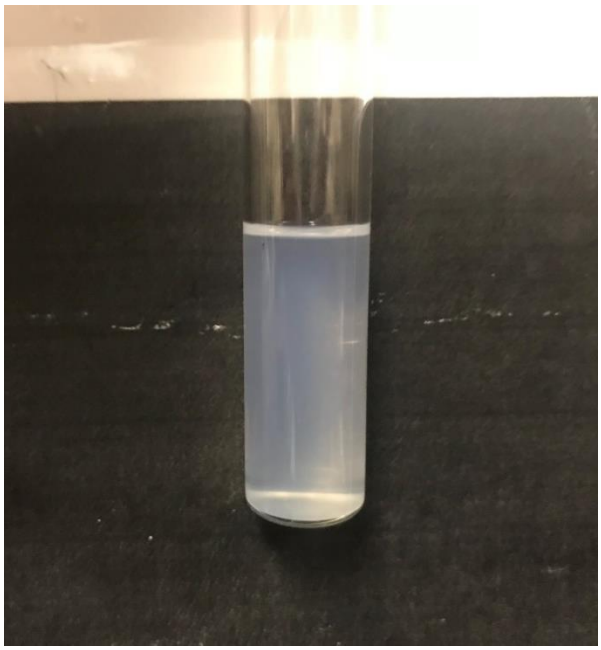

Figure. 34. Example of Precipitation Sample of Stability Test

Table. 2. Summary of Phase Behavior of Case 1 (Surfactant only)

Hydrocarbon	Heptane	Octane	Decane	Dodecane
S^*	0.7	0.9	1.3	1.7
Type III range	0.7	0.9	1.2-1.4	1.7-1.8
Coalescent rate of type III	8 min	5 min	12 min	6 min

Table. 3. Summary of Phase Behavior of Case 2 (5% urea)

Hydrocarbon	Heptane	Octane	Decane	Dodecane
S^*	1.2	1.4	2	2.4
Type III range	1.1-1.3	1.4-1.6	1.6-2.3	1.8-2.6
Coalescent rate of type III	6 min	3.5 min	6.5 min	2.5 min
S^* Increase	71.40%	55.60%	53.80%	41.20%

Table. 4. Summary of Phase Behavior of Case 3 (NaXS)

Hydrocarbon	Heptane	Heptane	Heptane	Dodecane
NaXS conc.	5%	1%	0.50%	1%
S^*	N/A	0.4	0.6	1.7
Type III range	0	0.3-0.7	0.5-0.8	1.7-2.4
Coalescent rate of type III	7 min	5 min	5 min	6 min
S^* Decrease	N/A	60%	15.70%	0.00%

In summary, 5% urea has the best stability among these three cases. When mixing with the oil phase, samples contain 5% urea will be stable up to 2 months. Even the surfactant with an aqueous urea phase is stable up to one week. Samples with NaXS will be stable at a higher temperature. If the oil site requires an elevated temperature but low salinity formulation, NaXS as well as surfactant system should be suitable.

Both addition of urea and NaXS provide a more extensive and clear type III microemulsions, an addition of 5% urea will result in up to 70% optimum salinity increase compare with the surfactant only case. On the contrary, introduce NaXS into the system will reduce the optimum salinity. The optimum salinity shifts more with more NaXS added. For instance, 5% of NaXS shift the microemulsion to all type II from zero to 2 wt.% NaCl, while 0.5% NaXS only reduce the optimum salinity of 16% (from 0.7 wt.% to 0.6 wt.%).

Solubilization Parameter

Another study is done on the solubilization parameter as shown in **Figure 35**. Here is an example of decane salinity scan with 5% Urea added. Interfacial tension and solubilization parameter of oil and water have been calculated and shown with the matching salinity. Solubilization parameter is plotted; in a unit of the milliliter per gram. In other words, oil solubilization parameter is calculated based on the milliliter of oil dissolved in the gram of water phase, while the water solubilization parameter is the amount of water dissolved in the oil phase.

The R ratio of type I is less than 1; type 2 is greater than 1, and type III is equal to1. R ratio is defined as the cohesive energy per unit area between the surfactant and oil divided by the cohesive energy per unit area between the surfactant and the water phase. Thus, in type III microemulsion, the surfactant-oil and surfactant-water interactions are equal. By adding urea, the entire system becomes more hydrophilic which also changed the interactions. More hydrophilic means optimal salt level required is increased; it needs more salt to reach equilibrium.

The salinity of 1.3 wt.% sample is the optimum salinity in no urea case. However, the samples contain 1.3 wt.% NaCl is still in the Type I range after adding urea. This means either the interaction of surfactant and water increased, or the oil and surfactant interaction decreased.

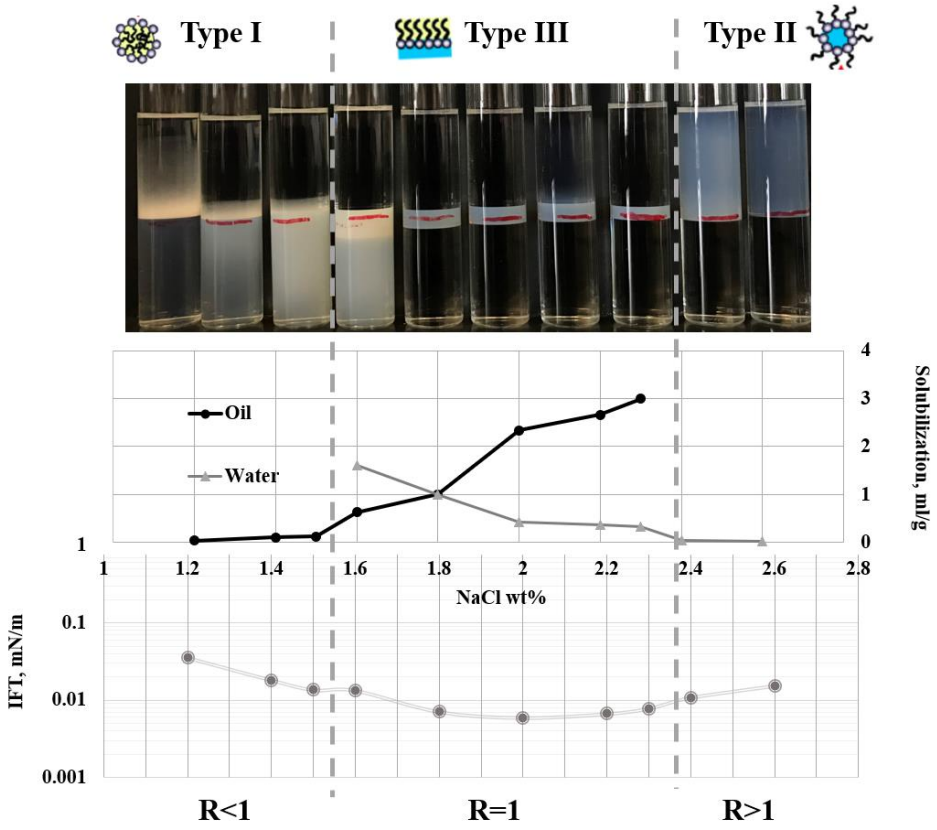

Figure 35. Solubilization Parameter and Interfacial Tension of AOT and SDBS with 5% Urea Mixed with Decane.

Adsorption study

Activated carbon, Indiana limestone, and Ottawa sand are chosen as the sand/soil. These sand is mixing with SDBS solutions for 72-hr equilibrium time separately. The 0.2 um filter and centrifuge are needed to keep the solution clear and clean for UV-Vis. Case 1 is still the SDBS only case with DI water; case 2 is SDBS mixing with 5% urea and case 3 is SDBS mixing with 1% NaXS solution.

Ottawa sand is clean and uniformed silica sand. According to the zeta potential measurements from Mukul M. Sharma and his group, Ottawa sand is negatively charged in the water solution (Sharma et al. 1987). However, the surface charge of mineral in the water depends on the pH; the neutral solution is giving a close to neutral surface charge as well. Then, limestone mainly contains calcite which is carbonates, the surface charge of limestone can be positively charged from pH 5 to pH 13 based on the result by Schramm and his group (Schramm et al. 1991). The surface area has also been reported, silica fines have 4.3 m^2 per gram, while the limestone has around 10.4m^2 per gram. Ottawa sand (left), Indiana limestone (middle) and Activated Carbon (right) with US Dime is shown in **Figure. 36**

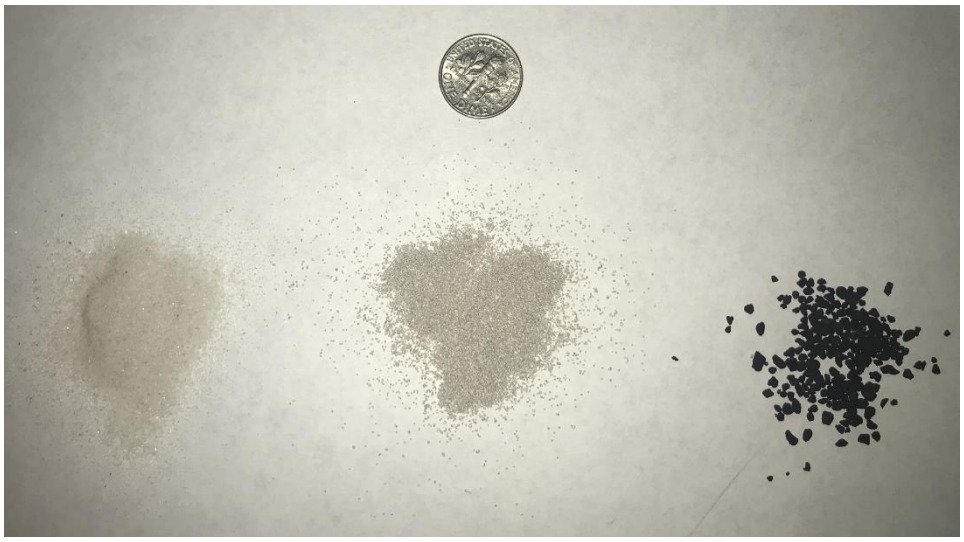

Figure. 36. Ottawa sand (left), Indiana limestone (middle) and Activated Carbon (right) with US Dime

The activated carbon adsorption samples are shown in **Figure 37**. from left to right, SDBS concentration is varying from 300 ppm to 1500 ppm. The figure gives an idea of how the adsorption changes the surfactant concentration in the aqueous phase. Activated carbon has a powerful absorbability, due to the large surface area (500-1700 m^2g^{-1}) and other physical properties. Thus after 72 hours, the foam is mainly disappearing as well as the aqueous solution becomes transparent.

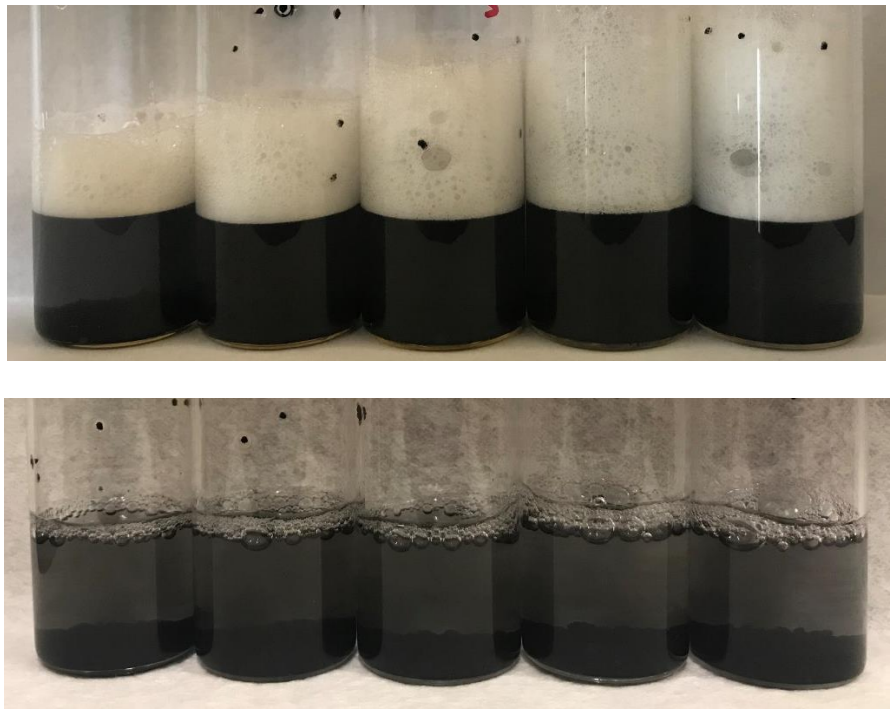

Figure 37. Comparison of Activated Carbon Samples Pre (Top) and Post (bottom) Adsorption.

The black activated carbon settled down on the bottom with some clay still in the upper aqueous phase and changed the color of the solution. The top photo was taken at the surfactant solution mix with activated carbon. The bottom photo was taken after 72-hr equilibrium time. However, for the clean Ottawa sand, the adsorption amount cannot be differentiated by just observation of naked eyes. The foam generation amount of after adsorption is similar to the beginning of the adsorption process from the photo shown in **Figure 38** below.

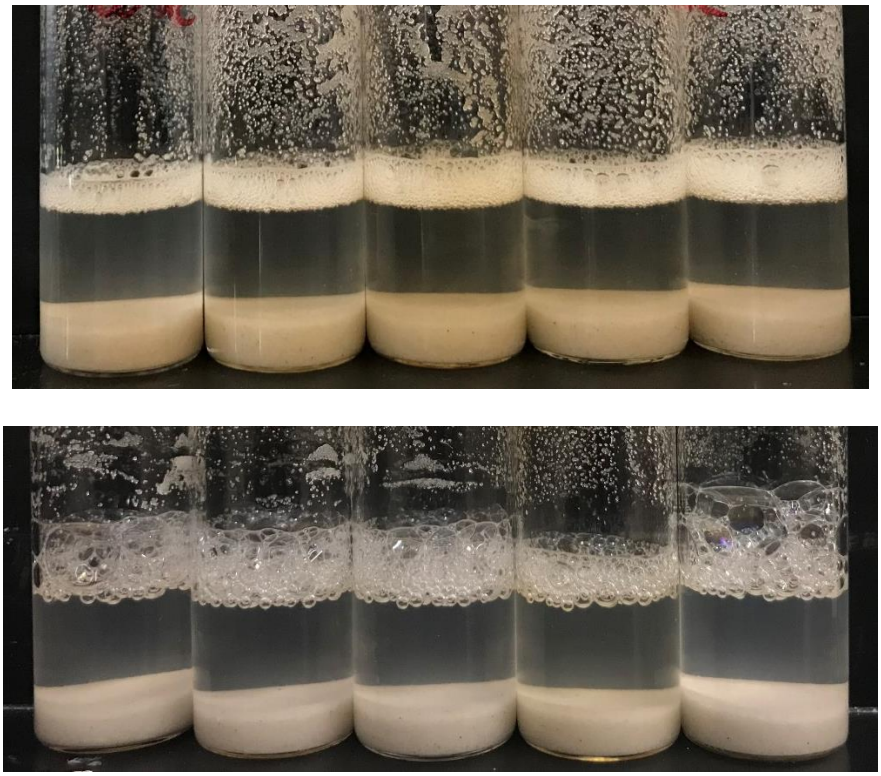

Figure 38. Comparison of Ottawa Sand Samples Pre (Top) and Post (bottom) Adsorption.

Adsorption amount has been calculated based on the UV-Vis absorbance on the 262 nm wavelength. The supernatant is taken from each sample, centrifugation for 20 minutes on the 6000 rpm is needed before the extract of the supernatant. Filtration is required primarily for the activated carbon samples since the black colored aqueous solution represent the suspension particles in the solution. Due to the working mechanism of UV-Vis being measuring the amount of light absorbed at the targeted wavelength, the color of the solution and the suspended solids will influence the result. The results of the three types of sand are present below. Adsorption of surfactant (SDBS) in milligram per gram of sand as a function of post concentration of SDBS in the unit of ppm.

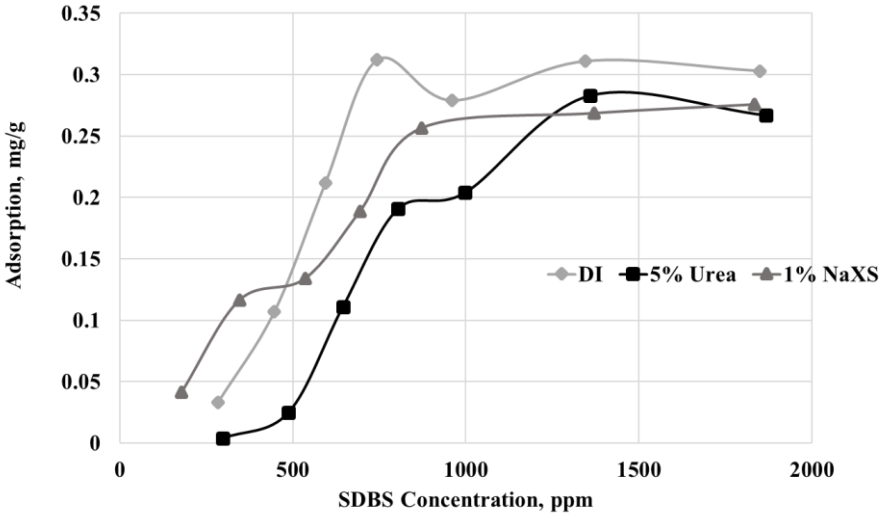

Figure 39. Adsorption Test of SDBS with Ottawa Sand

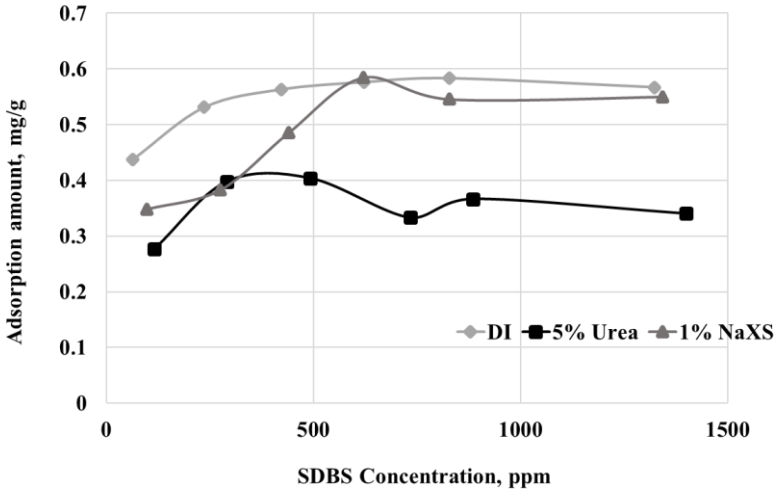

Figure 40. Adsorption Test of SDBS with Indiana Limestone

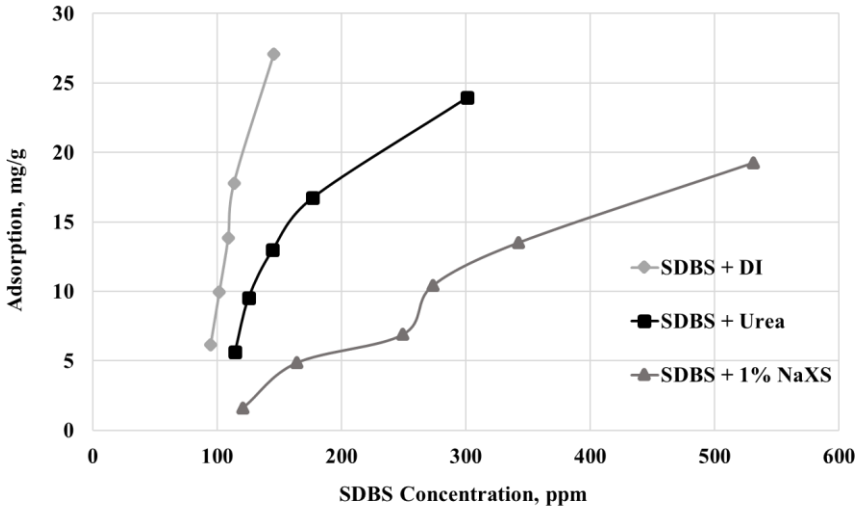

Figure 41. Adsorption Test of SDBS with Activated Carbon

Figures 39 - 41 are the adsorption study result of Ottawa sand, Indiana limestone, and activated carbon, respectively. By adding urea, there is an apparent reduction of surfactant adsorption for all three types of sand. Addition of NaXS results in reducing the adsorption amount of Ottawa sand and activated carbon but no significant change for the Indiana limestone. The reduction percentage is calculated of each concentration and average of all concentration and concentration beyond CMC is shown in **Tables 5** and **6.**

Table. 5 Adsorption Reduction by Adding Urea

	Ottawa Sand	Indiana Limestone	Activated Carbon
Average Reduction	42.67%	34.98%	7.16%
Average Reduction above CMC	21.64%	34.66%	N/A

Table. 6 Adsorption Reduction by Adding NaXS

	Ottawa Sand	Indiana Limestone	Activated Carbon
Average Reduction	7.44%	12.19%	53.44%
Average Reduction above CMC	13.61%	3.68%	N/A

The critical micelle concentration (CMC) of SDBS is around 650 ppm based on the surface tension measurement in Figure 42. For case 1 (Ottawa sand), the CMC of SDBS is approximately 650 ppm when the plateau is reached. After introducing 5% urea into the SDBS solution, the CMC increased, and the plateau is being put off to around 1000 ppm. The reason why CMC increased should be the aqueous phase structure changed. It became harder to form micelle due to the surface tension, and chemical bonding between water molecule changed. In the literature, by adding hydrotrope, the radius of the water molecule changed. Then, after adding 1% NaXS, the reduction of adsorption amount is also observed after 500 ppm of SDBS concentration. Moreover, Ottawa sand adsorption amount is traces. The maximum value is around 0.32 mg/g, which is reasonable because of the uniformed particle size, clean sand constitution, and limited surface area.

Then, for the second case (Indiana limestone), the adsorption amount of SDBS only case become flat at the very early time (500 ppm). And the urea one display a significant reduction of absorbed of SDBS in solution. Approximately, 40% reduction is observed after CMC. This result gives a new insight into the surfactant flooding system. It can contribute to solve the surfactant loss of adsorption on reservoir rock

and control economically on the spendings on chemicals purchase.

On the contrary, the addition of NaXS did not show a significant drop of adsorption amount of SDBS. It has some effect on reducing the adsorption in the lower concentration (less than 620 ppm) but when reaches the CMC, the result has been weakening and becoming similar to the DI water case. This can be the effect of the surface charge of Indiana limestone in the water, the positively charged sand face in contact with the anionic surfactant solution, the interaction between them may be an issue.

Lastly, the activated carbon case, both urea, and NaXS solution show a reduction on the SDBS adsorption. Only 0.5g of AC is added into 10g of surfactant solution due to the strong adsorption ability. The tendency of these three lines are quite dissimilar, NaXS added case is the flattest one. Unlike the previous two cases, Indiana limestone displays the best ability to reducing the surfactant loss. When examining the supernatant samples, there is an interesting phenomenon being found. The loss of hydrotrope itself may influence the adsorption result. In this activated carbon case, when determining the concentration of SDBS in the post solution. Approximately 60% of NaXS is disappeared after adsorption, while this phenomenon is not detecting in any other cases. This unaccounted part of NaXS may be adsorbed onto the sand surface first and occupied the limited area. Then, influence the SDBS adsorption and decrease the surfactant loss.

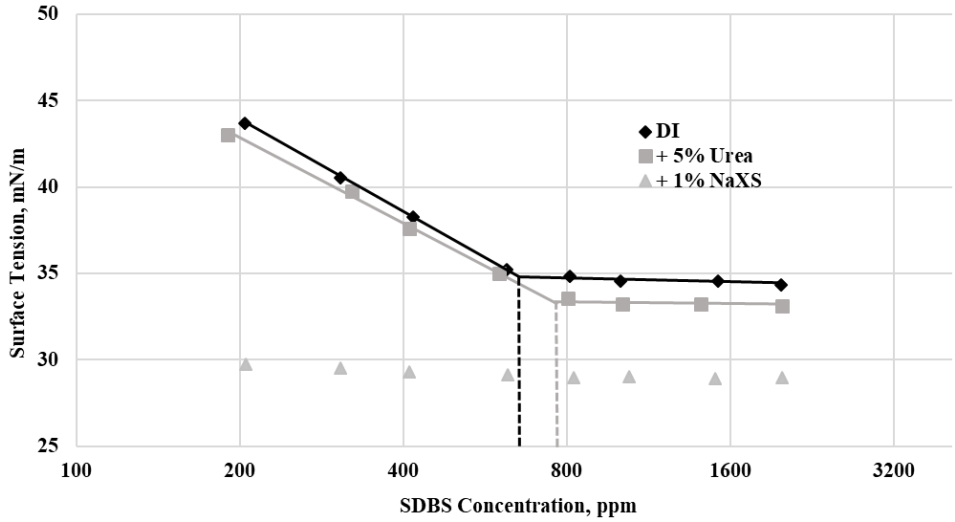

Figure 42. Surface Tension Measurement SDBS with DI and SDBS with 5% urea and 1% NaXS added, measured by pendant drop method.

To ensure the integrity of adsorption results, the surface tension of each solution is tested using the pendant drop method mentioned in the previous section. The result is shown in Figure 42 where the x-axis is SDBS concentration in parts per million in a log scale and the y-axis is the measurements of surface tension. The black rhombic dots stand for the SDBS with DI water solution; gray square dots are SDBS with 5% urea solution and the triangular dots on the bottom represents SDBS with 1% NaXS added. Four straight line is marked to calculate the CMC value of SDBS and SDBS with urea case. The CMC is reported to be 650 ppm and 775 ppm. Thus, the addition of 5% urea increases the CMC of 125 ppm which is roughly 19% increase. This surface tension measurement supports the adsorption test result that by adding urea, CMC of SDBS increase.

Due to the NaXS has surface active ability itself and the effect on SDBS solution, the surface tension measurements are all around 29 mN/m even on the 200 ppm SDBS

solution. This may also because of the error due to the low surface tension, which caused the pendant drop not to form the familiar pendant shape; instead, the droplet sticks to the outside surface of the needle and become build up the volume on it. An example of this phenomenon shown in **Figure 43**. This unusual fact is changing the shape of the droplet and cause the software analysis the changed shape of the droplet. This error caused the surface tension measurement not reliable for this case.

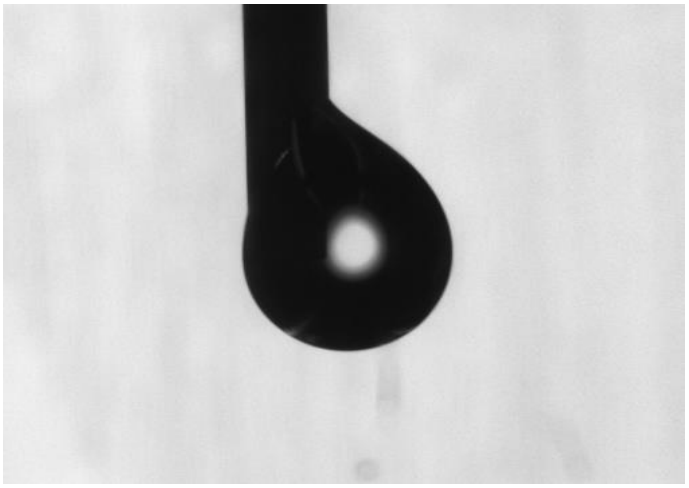

Figure. 43. Droplet of SDBS with NaXS Solution on the Needle surface

V. Conclusions

A significant economic barrier to the widespread use of the surfactant flooding technology is the loss of surfactant through adsorption on aquifer and reservoir minerals. Especially in the case of EOR in highly saline brines, losses of surfactant may be the most significant single expense in the application. In my study, with only adding 5% of Urea, we can reduce up to 43% of surfactant adsorption with Ottawa sand and 35% of Indiana limestone. For NaXS, the effect on surfactant adsorption is less practical on Ottawa sand and Indiana limestone, but for activated carbon, the reduction is up to 53%. Also, the addition of 5% urea, critical micelle concentration(CMC) increased.

As for phase behavior study, by adding 5 wt% of urea into the AOT/SDBS system, resulting in type III window becomes wider and middle phase becomes more transparent; S* increased up to 71%; coalescent rate improved. Stability issue with phase separation after adding oil phase is solved. Addition of 1% NaXS will shift the Type III microemulsion to the lower or no salinity range which gives the excellent potential for the low salinity reservoir condition. The 50 °C will fix the phase separation issue.

This study offers insights on the extent to which the addition of proper hydrotrope may help to formulate an efficient and low-cost surfactant flooding system.

Chapter II: Formulations of Microemulsions for Dense Non-Aqueous Phase Liquids: Effects of Soybean Oil Methyl Ester

I. Introduction:

A new solvent has been found in the 1990s, extract from soybean oil, which named SoyGold. The primary compounds of SoyGold are fatty acid methyl esters, and some types of SoyGold also contains surfactant depending on the targeted application. This light oil like fluid has been widely used as a solvent on bioremediation of groundwater and soil. SoyGold also is put in cleaners in our daily life, such as hand cleaner and nail polish remover (Chempoint). SoyGold is an environmentally friendly solvent compare to other petroleum-based ones. It is 100% biodegradable, has a higher solvent strength and a lower volatile organic compound (VOC) (Chempoint).

Groundwater is a valuable resource that is used for drinking water in many countries all over the world (Feld et al. 2016). Polluted groundwater aquifers used for drinking water are often remediated by use of the pump-and-treat technology, where the water is pumped up and treated at the site, typically by adsorption of the contaminants onto activated carbon (Benner et al. 2013; Feld et al. 2016). However, a new treatment approach of injecting SoyGold straightforward into the subsurface is found. By pumping SoyGold into the underground, it will not only benefit the bioremediation on the contaminated phase, but also it will contribute to the buoyancy and density adjustments. In the oil industry, this new solvent will offer significant assistance on mobilizing the dense non-aqueous phase liquid (DNAPL) in the subsurface.

Bioremediation

Bioremediation is a process of using the naturally occurring bacteria to remediate contaminants in soil and groundwater (Gundling). SoyGold is used during this bioremediation process to optimizes the subsurface environment by beneficial bacteria growth. The illustration (**Figure 44**) shows the SoyGold working process during the groundwater bioremediation. SoyGold is injected into the subsurface, and it will provide the nutrition for bacteria to consume. Then the enzymes which released by the bacteria will break down the contaminations of groundwater (Gundling).

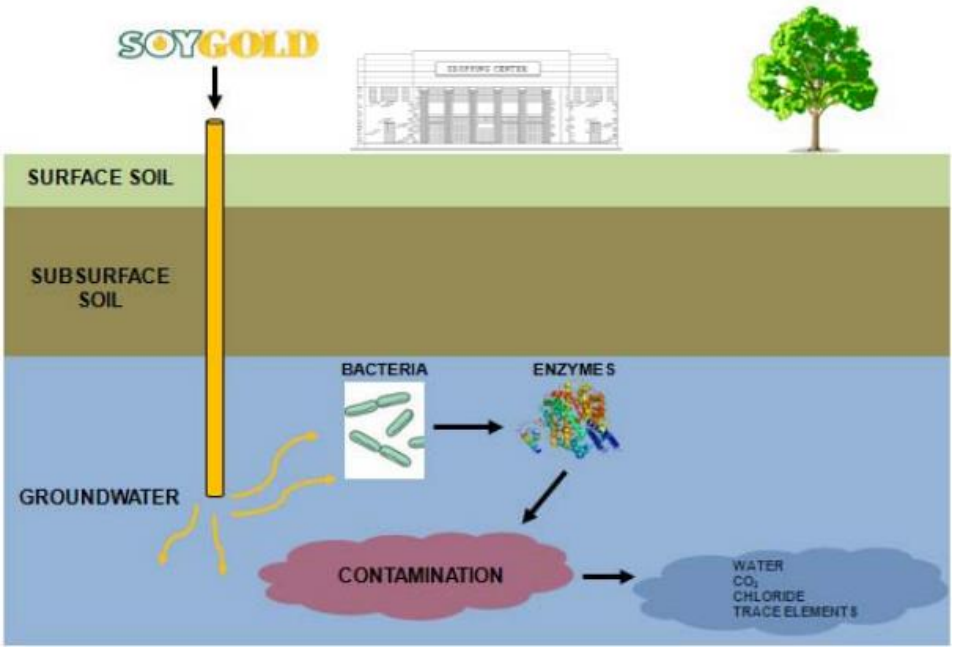

Figure 44. Illustration of SoyGold Working Process During the Groundwater Bioremediation (Gundling).

Fatty acid methyl esters (FAME)

Fatty Acid Methyl Esters (FAME) are esters of fatty acids. The physical characteristics of fatty acid esters are closer to those of fossil diesel fuels than pure vegetable oils, but properties depend on the type of vegetable oil (European Biofuels). FAME has physical properties similar to those of conventional diesel. It is also non-toxic and biodegradable (European Biofuels). FAME is produced from vegetable oils, animal fats or waste cooking oils by transesterification. The production reaction of FAME biodiesel is shown in **Figure 45**. with the help of methanol. glyceride reacts with an alcohol in the presence of a catalyst, forming a mixture of fatty acids esters and an alcohol (European Biofuels). SoyGold is produced in this method and can be considered as the biodiesel.

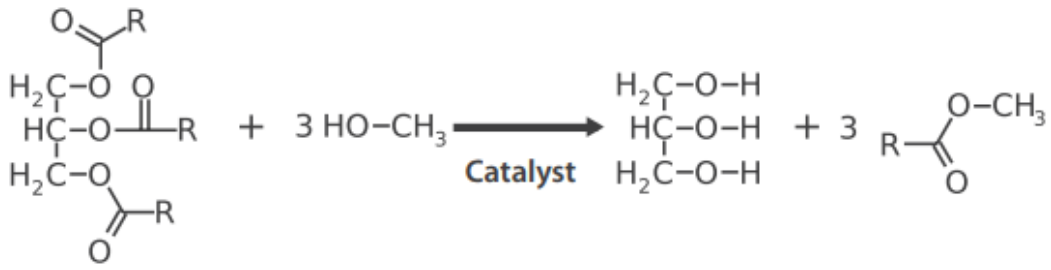

Figure 45. The reaction of producing FAME (European Biofuels)

Dense non-aqueous phase liquids (DNAPLs)

Dense non-aqueous phase liquids (DNAPLs) is a type of chemicals or mixtures of compounds that have two primary characteristics in common: they are heavier than water, and they are only slightly soluble in water (CLU-IN). Due to the physical characteristics of DNAPL, they may form the separate non-aqueous phase in the subsurface (ITRC 2015). The mobility characteristics of DNAPL is discussed in Figure 46. which adopted from ITRC (Interstate Technology & Regulatory Council) website.

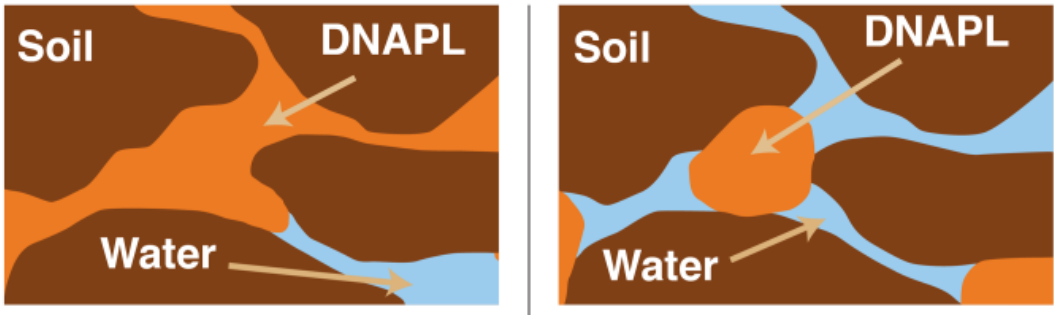

Figure 46. The mobility characteristics of DNAPL. Mobile and potentially mobile DNAPL(left) and Immobile residual phase DNAPL(right) (ITRC 2015)

In the illustration, the orange portion represents the DNAPL, and it is located in the porous media of the reservoir rock. The mobile DNAPL has the continuous shape in the pore, and it is able to migrate. The potentially mobile DNAPL is also in the similar form of mobile DNAPL; however, the capillary pressure is not exceeding the groundwater pore pressure. It can be mobilized with the change of pore conditions. The immobile residual phase DNAPL is shown on the right of **Figure 46**. It cannot be mobilized due to the capillary pressure limitation (ITRC 2015).

II. Objective

Three types of SoyGold samples are chosen in this study. A prediction of the equivalent alkane carbon number (EACN) is needed before examining the SoyGold effect on DNAPL phase behavior. Trichloroethylene (TCE) is the DNAPL phase selected and measured the EACN for comparison. To examine the SoyGold effect on DNAPL phase, phase behavior study of a SoyGold and TCE mixture is needed and IFT data also measured by the spinning drop tensiometer. Density adjustments and viscosity measurements are also provided. The newly developed system, which adds SoyGold into the TCE, should create a stable type III microemulsion with a selected surfactant system. Density and stability of mobilized DNAPLs produced by the new surfactant formulations should be significantly improved to safely catching and recovering through the recovery wells.

III. Materials & Methods

Materials

Three types of SoyGold is selected. The comparison of them are listed in **Table 7.** The information is adopted from the Chempoint website (Chempoint). They are all vegetable oil has the light-yellow color and the same density. The viscosity values are different by observation in the test tube and the SoyGold 2000 has the most yellowish color among them.

Table 7. Comparisons of various SoyGold Products

SoyGold	Description	Density, g/ml
1000	Methyl ester, soybean oil 100%	0.88
1100	Methyl ester, soybean oil 100%	0.88
2000	Methyl ester, soybean oil 95-99%, nonionic surfactant 1-5%	0.88

The hydrocarbons used in this study is listed in **Table 8**. The physical properties of them are also provided.

Table 8. Hydrocarbon Tested

Name	Chemical formula	Density, g/ml	molecular weight, g/mol
TCE	C_2HCl_3	1.46	131.38
Octane	C_8H_{18}	0.702	114.23
Dodecane	$C_{12}H_{26}$	0.75	170.34

Methods

In this chapter, phase behavior study and interfacial tension measurements of the SoyGold samples are also utilized in the same procedures as in the previous chapter. Coalescence rate and the location of the middle phase in the type III microemulsion phase behavior samples are compared and used to determine the optimum salinity case.

The viscosity data is obtained from the dropping-ball viscometer. The solution been prepared first and filled up the glass tube. No bubble is allowed in the tube, and the glass ball is placed in the tube before sealed. Place the viscometer vertically and observe the glass ball dropping. Record the ball dropping time from the start line to the end line which marked on the glass tube and the viscosity of the fluid can be calculated.

IV. Results and Discussions

Prediction of the equivalent alkane carbon number (EACN)

The EACN of SoyGold 1000 is measured by the phase behavior study with extended surfactant (2.5 wt.% Alfoterra 8-41S). A 5ml of the surfactant solution is mixed with 5 ml of the oil phase (2.5ml of Dodecane and 2.5 ml of SoyGold 1000). Due to the low EACN of SoyGold, the EACN of the mixture contains SoyGold and dodecane is easier to be measured. The phase behavior samples are shown in **Figure 47** with selected salinity marked on top of each sample.

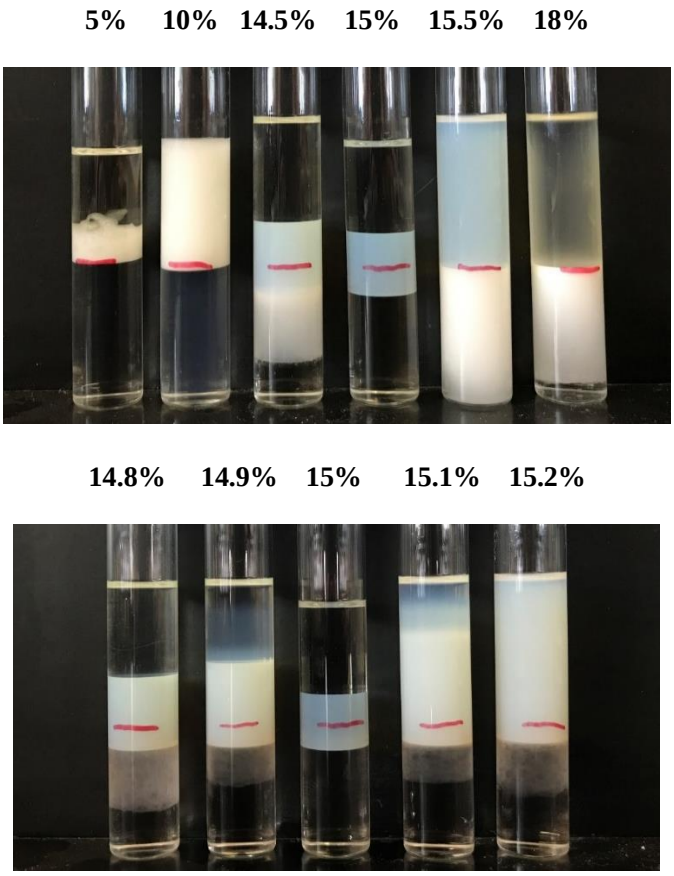

Figure 47. Phase behavior samples of SoyGold 1000 for EACN measurement in bigger salinity scan (top) and finer salinity scan (bottom)

Similarly, EACN is measured in the same method for SoyGold 1100 and 2000. The results are shown in **Figures 48** and **49**.

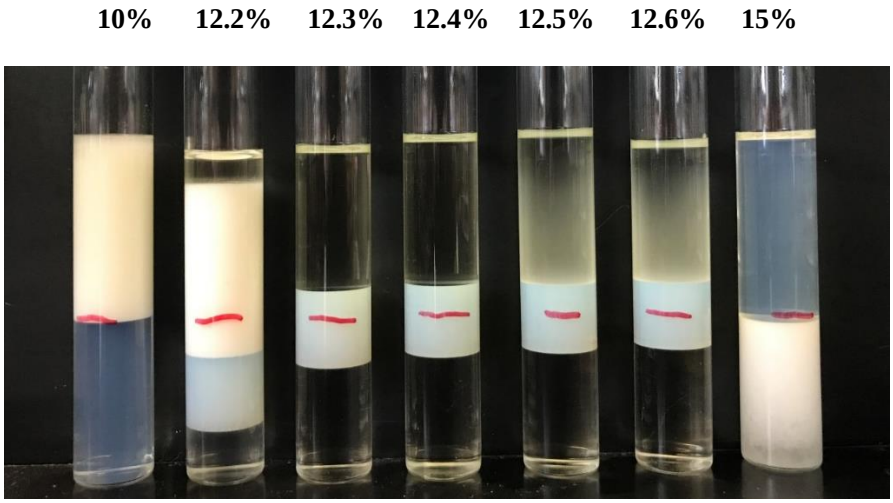

Figure 48. Phase behavior samples of SoyGold 1100 for EACN measurement

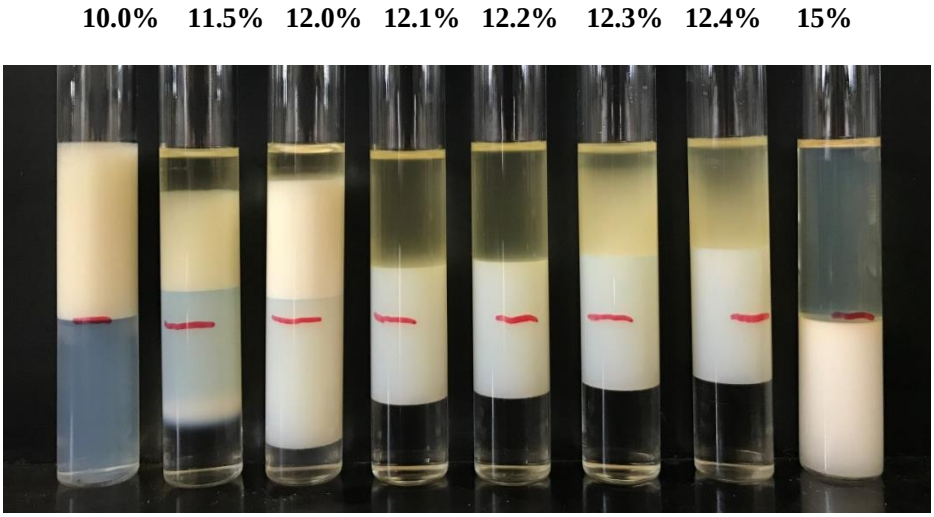

Figure 49. Phase behavior samples of SoyGold 2000 for EACN measurement

The optimum salinity of SoyGold 1000, 1100 and 2000 with dodecane mixtures are 15 wt.%, 12.4 wt.% and 12.2 wt.% from the observation of phase behavior samples. Then the EACN of the mixture is calculated based on the K and Cc value from

literature. Based on the 2.5wt% AF 8-41s K and Cc value, the equation below from Wei Wan is used, and EACN of the mixture is calculated to be 8.5 for the SoyGold 1000 and dodecane (Wan 2014).

$$ln(S^*) = 0.0478 * EACN + 2.4075 \quad (8)$$

$$EACN_{mix} = X_1 * EACN_1 + X_2 * EACN_2 \quad (9)$$

Where X1 is the mole fraction of dodecane (0.59), EACN1 equals 12 and X2 is the mole fraction of SoyGold 1000 (0.41). The mole amount of each type of oil can be calculated by the weight divided by the molecular weight of each one. Then, the mole fraction is calculated by the mole amount of each type of oil taken place in the oil mixture. Then, according to linear mixing rule, the EACN of SoyGold 1000 is calculated to be 3.46 based on Eq 9 and the related properties. Similarly, EACN of SoyGold 1100 and 2000 is estimated to be 4.10 and 3.73. An IFT measurement is also provided to ensure the result of the optimum salinity (**Figure 50**).

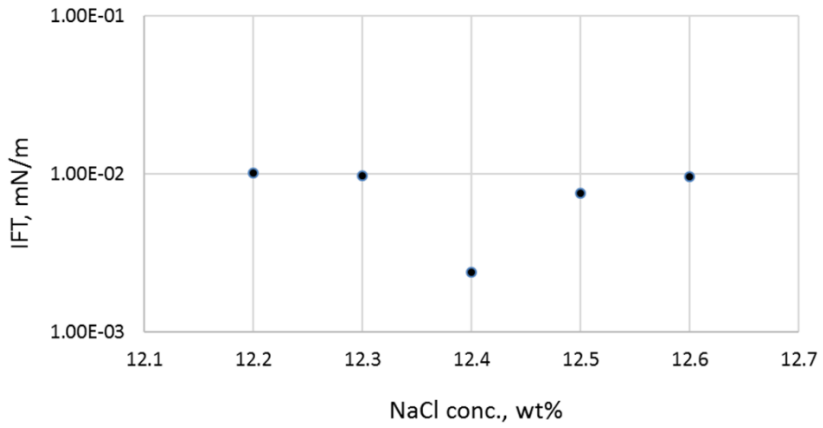

Figure 50. IFT measurement of phase behavior sample of SoyGold 1100 and dodecane

After predicting the EACN of three types of SoyGold, TCE is also been tested and measured. The samples are shown in **Figure 51**.

10% 12.5% 13.5% 15% 15.3% 15.5% 15.7% 16% 17.5%

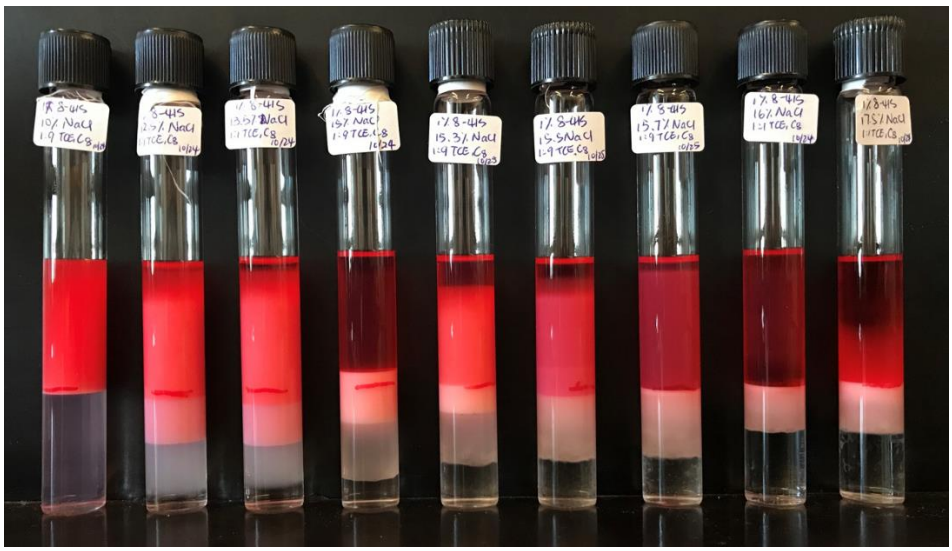

Figure 51. Phase behavior samples of TCE and Octane (1:9 ratio) for EACN measurement

In this case, TCE is dyed using Sudan red powder due to the high toxicity. After TCE solution is dyed to red color, it is easy to be found if any TCE is spilled. Again, due to the low EACN number of TCE, a 1 to 9 ratio of TCE and octane is used in the EACN measurement. The mixture of oils is being stirred with a magnetic bar in the solution for 24 hours of equilibration period. The optimum salinity is observed to be 15 wt.%, and the EACN of TCE is estimated to be -2.07.

Density alteration of SoyGold and TCE mixture

Before doing the phase behavior study of the mixture contains SoyGold and TCE, a density adjustment is needed to determine the optimum case which the density is lighter than the aqueous phase. SoyGold 1100 is selected as the optimum SoyGold due to the fast coalescence rate compared to other SoyGold samples. The ratio of SoyGold/TCE and the density measurements are shown in **Table 9**. The volume ratio of TCE and SoyGold 1100 of 2 to 8 is selected.

Table 9. Density adjustment of SoyGold and TCE mixture

Volume Ratio		Density
TCE	SoyGold 1100	g/cm^3
2	8	0.98
3	7	1.03
4	6	1.09
5	5	1.16
6	4	1.2
7	3	1.27
8	2	1.32
9	1	1.39

Phase behavior study of SoyGold 1100 and TCE mixture

The selected surfactant solution with AOT/Calfax and mixed with the 2 to 8 ratio mixtures of TCE and SoyGold 1100. A wider salt window for type III microemulsions is realized in the **Figure 52**. The middle phase is thin and cloudy. The IFT measurement is provided in **Figure 53**. A large range of ultra-low IFT is detected from salinity of 1wt.% to 4 wt.%.

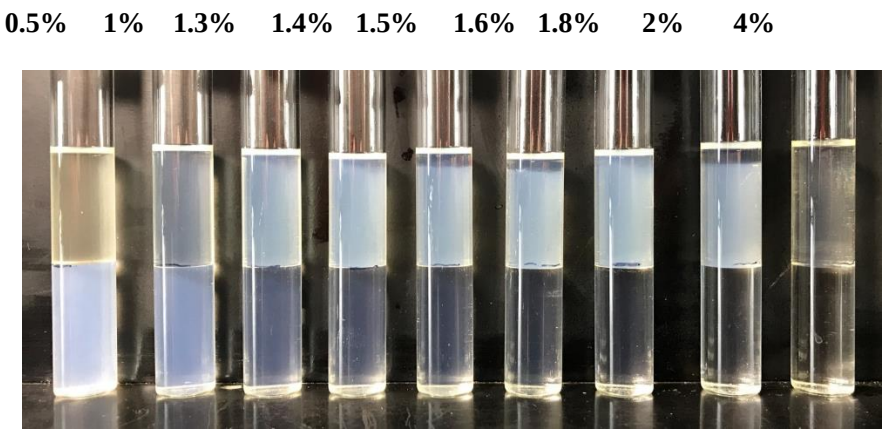

Figure 52. Phase behavior samples of SoyGold 1100 and TCE mixture

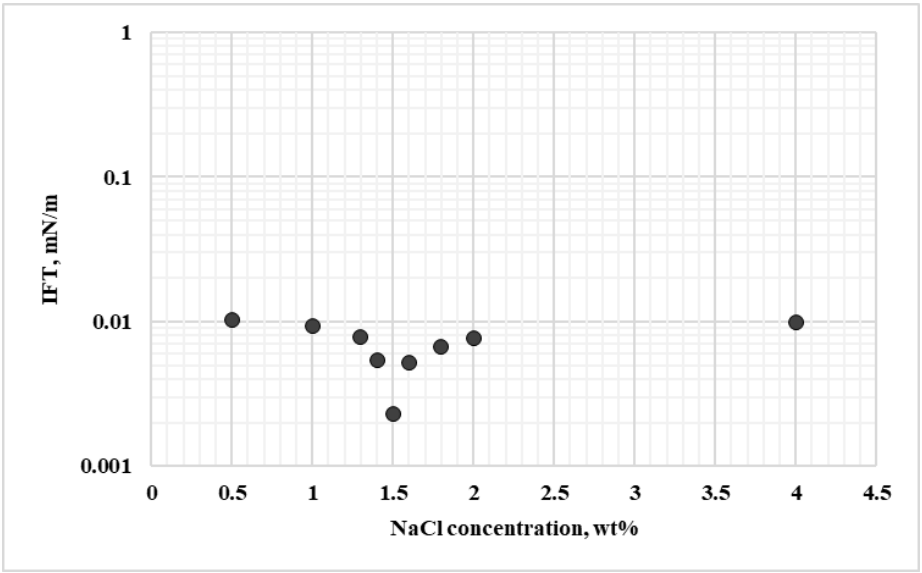

Figure 53. IFT measurement of phase behavior samples of SoyGold 1100 and TCE mixture

Stability test with Viscosity measurement

To examine the stability of the SoyGold and TCE mixtures, a stability test with the viscosity measurement is needed. Xanthan Gum is used to improve the viscosity and stability of the samples. The samples contain 5ml of aqueous solution and 5ml of SoyGold 1100; another set of the samples contains addition of 2ml of TCE. Four set of samples are prepared and shown in **Figure 54, 55**. and **Table 10.**

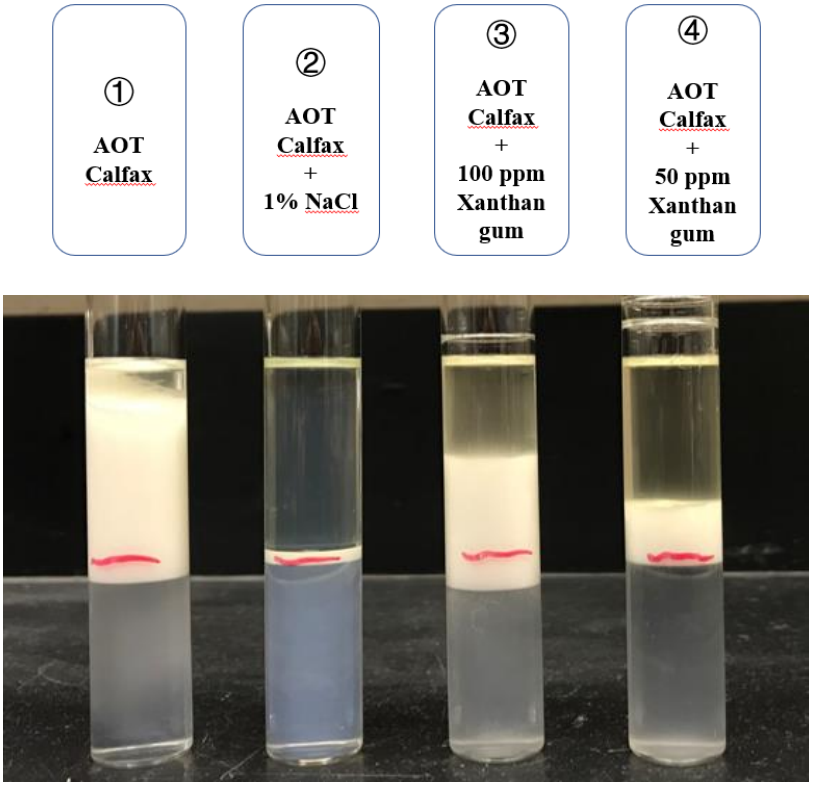

Figure 54. Stability test samples with 5ml SoyGold 1100

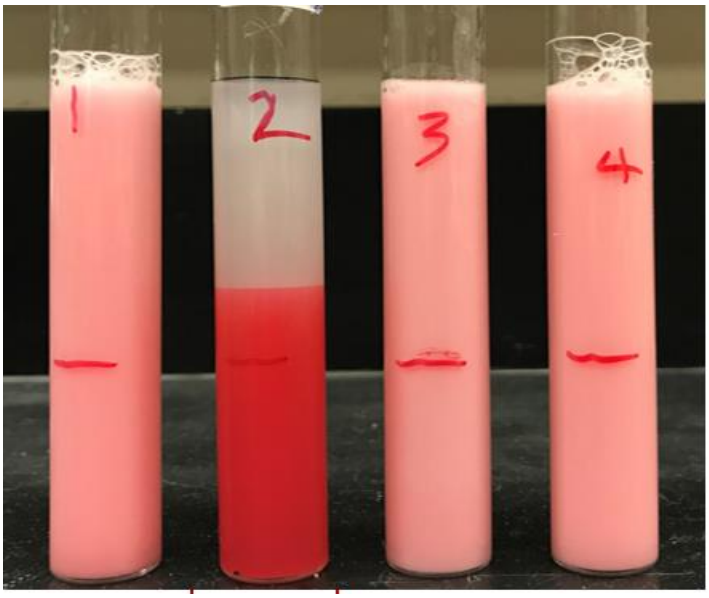

Figure 55. stability test samples with 5ml SoyGold 1100 and 2ml TCE

Table 10. Viscosity measurements in centipoises

Sample	①	②	③	④
	Surfactant only	With 1% NaCl	With 100pm Xanthan Gum	With 50 ppm Xanthan Gum
With 5ml SoyGold	2	4.05	12.92	12.3
With 5ml SoyGold and 2ml TCE	2.98	1.73	10.4	6.73

After manually mixing, sample 1 and 2 are separated after 6 to 12 minutes. However, in addition of xanthan gum, the stability is improved up to 12 hours as well as the viscosity increased. This study offers a lot of possibilities of this co-solvent formulation on other heavier DNAPLs which can benefit the mobility and stability of the fluids.

V. Conclusion

SoyGold 1100 can be used on the density adjustment of DNAPL phase, and it can provide a broad and stable type III microemulsion which has an ultra-low interfacial tension in low salinity range (less than 4 wt.% NaCl). With the injecting SoyGold straightforward into the subsurface, the DNAPL phase that trapped in the pore can be solubilized and mobilized with the aqueous phase. By pumping SoyGold into the underground, it will not only benefit the bioremediation on the contaminations, but also it will contribute to the buoyancy and density adjustments and then assistance on mobilizing the residual dense non-aqueous phase liquid (DNAPL) in the subsurface.

Reference

Abriola, L. 2002. Surfactant Enhanced DNAPL Source Zone Remediation: Results of a Field Demonstration and Implications for Bioavailability. Chicago, Illinois, 10—12 December.

Balasubramanian, V.S., Gaikar, V.G., and Sharma, M.M. 1989. Aggregation Behavior of Hydrotropic Compounds in Aqueous Solution. J. Phys. Chem 93: 3865—3870.

Bera, A., Kumar, T., Ojha, K. et al. 2013. Adsorption of surfactants on sand surface in enhanced oil recovery: Isotherms, kinetics and thermodynamic studies. *Applied Surface Science* 284: 87—99.

Benner, J., Helbling, D.E., Kohler, H. et al. 2013. Is biological treatment a viable alternative for micropollutant removal in drinking water treatment processes? Water Res 47:5955–5976. doi: 10.1016/j.watres.2013.07.015.

Biolin Scientific. Attension Theta, https://www.biolinscientific.com/attension/optical-tensiometers/theta (accessed 15 May 2018).

Bourrel, M. and Schechter, R.S. 1988. The R-ratio. In *Microemulsions and Related Systems: Formulation, Solvency, and Physical Properties*. New York, New York: Marcel Dekker.

Chempoint, Soy Methyl Esters Are An Environmentally Friendly, Biodegradable and effective, https://go.chempoint.com/SoyGoldSolvent (accessed 08 October 2018).

Clark, J. Chemguide. UV-VISIBLE ABSORPTION SPECTRA, https://www.chemguide.co.uk/analysis/uvvisible/theory.html

CLU-IN. Dense Nonaqueous Phase Liquids (DNAPLs) , https://clu-in.org/contaminantfocus/default.focus/sec/Dense_Nonaqueous_Phase_Liquids_(DNAPLs)/cat/Overview/ (accessed 10 September 2018).

Dhapte, V. and Mehta, P. 2015. Advances in hydrotropic solutions: An updated review. St. Petersburg Polytechnical University Journal: Physics and Mathematics 1 (4).

European Biofuels Technology Platform. Fatty Acid Methyl Esters (FAME), http://www.etipbioenergy.eu/images/fame-fact-sheet.pdf (accessed 11 October 2018).

Feld, L., Nielsen, T.K., Hansen, L.H. et al. 2016. Establishment of Bacterial Herbicide Degraders in a Rapid Sand Filter for Bioremediation of Phenoxypropionate-Polluted Groundwater. *Appl Environ Microbiol* 82 (3): 878—887

Gezer, A. and Karagunduz, A. 2011. Use of Surfactants in Soil and Groundwater Remediation. Survival and Sustainability: 995—1004.

Gundling, S. KU Resources. SoyGold Bioremediation Technology for Chlorinated Solvents , http://www.kuresources.com/wp-content/uploads/2016/02/SoyGold-Flyer-Commercial.pdf (accessed 11 October 2018).

ITRC (Interstate Technology & Regulatory Council). 2015. Integrated DNAPL Site Characterization and Tools Selection (ISC-1). Washington, D.C.: Interstate Technology & Regulatory Council, DNAPL Site Characterization Team. www.itrcweb.org/DNAPL-ISC_tools-selection.

Johnson, J. Truth in Aging. Sodium Xylene Sulfonate https://www.truthinaging.com/ingredients/sodium-xylene-sulfonate (accessed 03 April 2018).

Lorna, L. Hair Momentum. Types of surfactants in your shampoo, http://hairmomentum.com/types-of-surfactants-in-shampoo/ (accessed 15 August 2018).

Jin, L., Budhathoki, M., and Jamili, A. et al. 2017. Predicting microemulsion phase behavior using physics based HLD-NAC equation of state for surfactant flooding. Journal of Petroleum Science and Engineering 151: 213—223.

Jin, L., Jamili, A., and Li, Z. et al. 2015. Physics based HLD–NAC phase behavior model for surfactant/crude oil/brine systems. Journal of Petroleum Science and Engineering 136: 68—77.

Johnson, S.C. Whats Inside Scjohnson. Sodium Xylene Sulfonate, https://www.whatsinsidescjohnson.com/us/en/ingredients/sodium_xylene_sulfonate

(accessed 12 July 2018).

National Research Council. 1999. Groundwater and Soil Cleanup: Improving Management of Persistent Contaminants. Washington, DC: The National Academies Press. https://doi.org/10.17226/9615.

Nidhi, K., Indrajeet, S., Khushboo, M. et al. 2011. HYDROTROPY: A PROMISING TOOL FOR SOLUBILITY ENHANCEMENT: A REVIEW. International Journal of Drug Development & Research 3 (2).

Nivas, B.T., Sabatini, D., Shiau, B. et al. 1996. Surfactant enhanced remediation of subsurface chromium contamination. Journal of Canadian Petroleum Technology 30 (3): 511—520.

Sakager, J.L., Morgan, J.C., and Schechter, R.S. 1979. Optimum Formulation of Surfactant/Water/Oil Systems for Minimum Interfacial Tension or Phase Behavior. SPE Journal 19 (2).

Qingdao IRO Surfactant Co., Ltd. IRO Surfactant. Sodium Dodecyl Benzene Sulphonate (SDBS, LAS), http://www.irosurfactant.com/LAS.htm(accessed 15 May 2018).

Sabatini, D., Knox, R., and Harwell, J. 1995. Surfactant-enhanced Subsurface Remediation: Emerging Technologies. American Chemical Society.

Salager, J.L. and Antón, R.E. 1999. Ionic Microemulsions. In *Handbook of Microemulsion Science and Technology*. New York, New York: Marcel Dekker.

Salager, J.L., Morgan, J.C., Schechter, R.S. et al. 1979. Optimum Formulation of Surfactant/Water/Oil Systems for Minimum Interfacial Tension or Phase Behavior. *SPE Journal* 19 (2): 107—115.

Schramm, L., Mannhardt , K., and Novosad, J.J. 1991. Electrokinetic properties of reservoir rock particles. *Colloids and Surfaces* 55: 309—331.

Sharma, M.M., Kuo, J., and Yen, T. 1987. Further Investigation of the Surface Charge Properties of Oxide Surfaces in Oil-Bearing Sands and Sandstones. *Journal of Colloid and Interface Science* 115 (1): 9—16.

Sheng, J.J. 2015. Status of surfactant EOR technology. *Petroleum* 1 (2): 97—105.

Som, I., Bhatia, K., and Yasir, M. 2012. Status of surfactants as penetration enhancers in transdermal drug delivery. J Pharm Bioallied Sci. 4 (1): 2—9.

Wan, W. 2014. Chemical Flood Under High Total Dissolved Solids (TDS) Conditions.

Wang, S., Yuan, Q., Kadhum, M. et al. 2018. In Situ Carbon Dioxide Generation for Improved Recovery: Part II. Concentrated Urea Solutions. Presented at the SPE Improved Oil Recovery Conference, Tulsa, Oklahoma.

Wei, X., Wang, X., Liu, J. et al. 2012. Adsorption kinetics of 3-alkoxy-2-hydroxypropyl trimethyl ammonium chloride at oil–water interface. *Applied Surface Science* 261 (15): 237—241.

Witthayapanyanon, A., Harwell, J., and Sabatini, D. 2008. Hydrophilic–lipophilic deviation (HLD) method for characterizing conventional and extended surfactants. Journal of Colloid and Interface Science: 259—266.